

Discontinuous Galerkin Methods for Computational Fluid Dynamics

B. Cockburn

*School of Mathematics, University of Minnesota,
Minneapolis, Minnesota 55455, U.S.A.*

ABSTRACT

The discontinuous Galerkin methods are locally conservative, high-order accurate, and robust methods that can easily handle elements of arbitrary shapes, irregular triangulations with hanging nodes, and polynomial approximations of different degrees in different elements. These properties, which render them ideal for *hp*-adaptivity in domains of complex geometry, have brought them to the main stream of computational fluid dynamics. In this paper, we study the properties of the DG methods as applied to a wide variety of problems including linear, symmetric hyperbolic systems, the Euler equations of gas dynamics, purely elliptic problems and the incompressible and compressible Navier-Stokes equations. In each instance, we discuss the main properties of the methods, display the mechanisms that make them work so well, and present numerical experiments showing their performance.

KEY WORDS: computational fluid dynamics, discontinuous finite elements

1. Introduction

This paper is a short essay on discontinuous Galerkin (DG) methods for fluid dynamics. The DG methods provide *discontinuous* approximations defined by using a Galerkin method *element by element*, the connection between the values of the approximation in different elements being established by the so-called *numerical traces*. Since the methods use discontinuous approximations, they can easily handle elements of arbitrary shapes, irregular triangulations with hanging nodes, and polynomial approximations of different degrees in different elements. The methods are thus ideally suited for *hp*-adaptivity in domains of complex geometry. Moreover, since they use a Galerkin method on each element, they can easily achieve high-order accuracy when the exact solution is smooth and high-resolution when it is not. Finally, when their numerical traces are properly chosen, they achieve a high degree of locality (and hence a high degree of parallelizability for time-dependent hyperbolic problems), they become locally conservative (a highly valued property in computational fluid dynamics), easy to solve and, last but not least, very stable even in the presence of discontinuities or strong gradients.

The first DG method was introduced by Reed and Hill (1973) for numerically solving the neutron transport equation, a linear hyperbolic equation for a scalar variable. Lesaint and Raviart (1974) recognized the relevance of the method and carried out its first theoretical

analysis. Since then, the method has been slowly evolving as it was applied to different problems. In the 90's, the method was successfully extended to non-linear time-dependent hyperbolic systems by Cockburn and Shu, see the review by Cockburn and Shu (2001), and since then the method has known a remarkably vigorous development. The purpose of this paper is to describe the method, discuss its main properties, uncover the mechanisms that make it work so well, and show its performance in a variety of problems in fluid dynamics.

The paper is organized as follows. In Section 2, we consider the original DG method for the neutron transport equation and its extension to linear, symmetric hyperbolic systems. In Section 3, we consider DG methods for non-linear hyperbolic conservation laws. In section 4, DG methods for second-order elliptic problems and, finally, in Section 5, DG methods for convection-dominated flows. Finally, we end in section 6 with some concluding remarks and bibliographical notes.

2. Linear hyperbolic problems

In this section, we begin by considering the DG method for numerically solving the neutron transport equation. It is in this framework that the idea of combining a Galerkin method on *each* element together with a *numerical trace* linking the different elements was introduced. We discuss the properties of local conservativity and local solvability of the method and show that the jumps of the approximate solution across inter-element boundaries *enhance* the stability of the method provided the numerical traces are properly defined. Moreover, we also show that these jumps are related to the *local residuals* in a linear fashion. This establishes a strong link between the DG method and the so-called stabilized methods. Finally, we extend the method to linear symmetric hyperbolic systems.

2.1. The original DG method

We begin by considering the original DG method of Reed and Hill (1973) which was devised to numerically solve the neutron transport equation,

$$\begin{aligned} \sigma u + \nabla \cdot (\mathbf{a} u) &= f && \text{in } \Omega, \\ u &= u_D && \text{on } \partial\Omega_-, \end{aligned}$$

where σ is a positive number, \mathbf{a} a constant vector and $\partial\Omega_-$ the *inflow* boundary of Ω , that is,

$$\partial\Omega_- = \{\mathbf{x} \in \partial\Omega : \mathbf{a} \cdot \mathbf{n}(\mathbf{x}) < 0\}.$$

Here $\mathbf{n}(\mathbf{x})$ is the outward unit normal at \mathbf{x} .

To define the method, we proceed as follows. First, we find the weak formulation the Galerkin procedure will be based upon. For each element K of the triangulation \mathcal{T}_h of the domain Ω , we multiply the neutron transport equation by a test function v and integrate over K to get

$$\sigma (u, v)_K - (u, \mathbf{a} \cdot \nabla v)_K + \langle \mathbf{a} \cdot \mathbf{n}_K u, v \rangle_{\partial K} = (f, v)_K \quad (1)$$

where \mathbf{n}_K is the outward unit normal to K ,

$$(u, v)_K = \int_K u v \, dx, \quad \text{and} \quad \langle w, v \rangle_{\partial K} = \int_{\partial K} w v \, ds.$$

This is the weak formulation with which we define the approximation to u , u_h . Thus, for each element $K \in \mathcal{T}_h$, we take $u_h|_K$ in the space of polynomials of degree k , $\mathbb{P}_k(K)$, and define it by requiring that

$$\sigma(u_h, v)_K - (u_h, \mathbf{a} \cdot \nabla v)_K + \langle \mathbf{a} \cdot \mathbf{n}_K \hat{u}_h, v \rangle_{\partial K} = (f, v)_K, \quad (2)$$

for all $v \in \mathbb{P}_k(K)$. Here, the numerical trace \hat{u}_h is given by

$$\hat{u}_h(\mathbf{x}) = \begin{cases} u_D(\mathbf{x}) & \text{for } \mathbf{x} \in \partial\Omega_-, \\ \lim_{\epsilon \downarrow 0} u_h(\mathbf{x} - \epsilon \mathbf{a}) & \text{otherwise.} \end{cases} \quad (3)$$

Note that if the vector \mathbf{a} is perpendicular to the normal \mathbf{n}_K , the above numerical trace is not well defined. However, the numerical trace of the flux $\mathbf{a} \cdot \mathbf{n}_K \hat{u}_h$, usually called the *numerical flux*, is actually well defined and is called the *upwinding numerical flux*. This completes the definition of the DG method.

Now, let us discuss some of the properties of this method. First, note that the fact that the numerical trace is well defined immediately implies that the DG method is a locally conservative method. This means that for any set S which is the union of elements $K \in \mathcal{T}_h$, we have

$$\sigma \int_S u_h dx + \int_{\partial S} \mathbf{a} \cdot \mathbf{n}_S \hat{u}_h ds = \int_S f dx.$$

This equation is obtained by simply taking $v = 1$ in the weak formulation (2) for each K in S and then adding the equations.

Next, note that the approximate solution can be efficiently computed in an element-by-element fashion. Indeed, from the weak formulation (2) and the definition of the numerical trace (3), we have

$$(\sigma u_h, v)_K - (u_h, \mathbf{a} \cdot \nabla v)_K + \langle \mathbf{a} \cdot \mathbf{n}_K u_h, v \rangle_{\partial K_+} = (f, v)_K - \langle \mathbf{a} \cdot \mathbf{n}_K \hat{u}_h, v \rangle_{\partial K_-},$$

where $\partial K_+ = \partial K \setminus \partial K_-$. Note that we have used the fact that, on ∂K_+ , $\hat{u}_h = u_h|_K$. Since the values of \hat{u}_h on ∂K_- do *not* involve values of $u_h|_K$, once u_h is known on the neighboring elements with edges on ∂K_- , we can easily compute u_h in K . An example is given in Fig. 1, where we can see that the approximate solution u_h on the elements of number i can only be computed after the approximate solution on the neighboring elements of number $j < i$ were obtained. Note that the approximate solution u_h on the elements with equal number can be computed simultaneously.

Let us now address the more delicate issue of the relation of the numerical trace with the stability of the method. First, let us establish a stability result for the exact solution of the neutron transport equation; we then use the procedure as a guide for dealing with the stability of the DG method. So, we take $v = u$ in the weak formulation of the exact solution (1) and obtain

$$\sigma(u, u)_K + \frac{1}{2} \langle 1, \mathbf{a} \cdot \mathbf{n}_K u^2 \rangle_{\partial K} = (f, u)_K.$$

Then, adding on the elements K , we get the equality

$$\sigma(u, u)_\Omega + \frac{1}{2} \langle 1, \mathbf{a} \cdot \mathbf{n} u^2 \rangle_{\partial\Omega_+} = (f, u)_\Omega - \frac{1}{2} \langle 1, \mathbf{a} \cdot \mathbf{n}_K u_D^2 \rangle_{\partial\Omega_-},$$

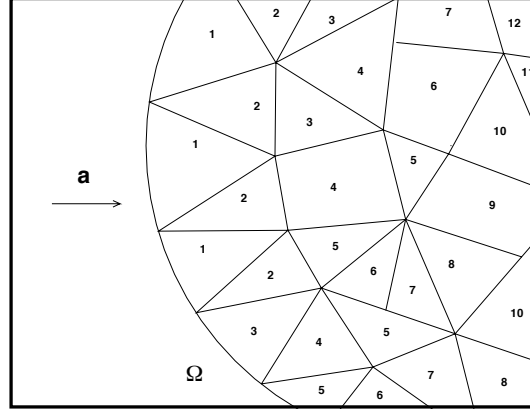


Figure 1. Solving the neutron transport equation with the DG method.

from which we immediately obtain

$$\|u\|_{\Omega}^2 := \sigma(u, u)_{\Omega} + \langle 1, |\mathbf{a} \cdot \mathbf{n}| u^2 \rangle_{\partial\Omega_+} \leq \frac{1}{\sigma}(f, f)_{\Omega} + \langle 1, |\mathbf{a} \cdot \mathbf{n}_K| u_D^2 \rangle_{\partial\Omega_-}. \quad (4)$$

Now, let us mimic this procedure to obtain a stability result for the DG method. We take $v = u_h$ in the weak formulation (2) and get

$$\sigma(u_h, u_h)_K + \frac{1}{2} \langle 1, \mathbf{a} \cdot \mathbf{n}_K \hat{u}_h^2 \rangle_{\partial K} + \Theta_K(u_h) = (f, u_h)_K,$$

where

$$\Theta_K(u_h) = -\frac{1}{2} \langle 1, \mathbf{a} \cdot \mathbf{n}_K (\hat{u}_h - u_h)^2 \rangle_{\partial K}.$$

If we add on the triangles K , we get the equality

$$\sigma(u_h, u_h)_{\Omega} + \frac{1}{2} \langle 1, |\mathbf{a} \cdot \mathbf{n}| \hat{u}_h^2 \rangle_{\partial\Omega_+} + \Theta_h(u_h) = (f, u_h)_{\Omega} + \frac{1}{2} \langle 1, |\mathbf{a} \cdot \mathbf{n}| u_D^2 \rangle_{\partial\Omega_-},$$

where

$$\Theta_h(u_h) = \sum_{K \in \mathcal{T}_h} \Theta_K(u_h),$$

from which we get

$$\|u_h\|_{\Omega}^2 + 2\Theta_h(u_h) \leq \frac{1}{\sigma}(f, f)_{\Omega} + \langle 1, |\mathbf{a} \cdot \mathbf{n}_K| u_D^2 \rangle_{\partial\Omega_-}. \quad (5)$$

The stability of the DG scheme would follow from the above inequality if $\Theta_h(u_h) \geq 0$. But this is indeed the case since

$$\Theta_h(u_h) = \frac{1}{2} \sum_{K \in \mathcal{T}_h} \langle 1, |\mathbf{a} \cdot \mathbf{n}_K| (\hat{u}_h - u_h)^2 \rangle_{\partial K_-} \geq 0,$$

by the definition of the numerical trace (3).

Let us further elaborate on this effect. If we compare the stability results (4) and (5), we immediately see that the stability of the DG method is *enhanced* by the presence of the term $2\Theta_h(u_h)$ containing the information about the size of the jumps of u_h across inter-element boundaries. This shows that the method exerts an automatic control on the size of the jumps. Moreover, it turns out that the size of the jumps is related to the ability of the method to solve the partial differential equation *inside* the element. To see this, note that the *local residual*,

$$R = \sigma u_h + \nabla \cdot (\mathbf{a} u_h) - f,$$

on the element $K \in \mathcal{T}_h$ is strongly related to the jumps of the approximate solution on ∂K . Indeed, a simple integration by parts in the weak formulation (2), reveals that

$$(R, v)_K = \langle \mathbf{a} \cdot \mathbf{n}_K (u_h - \hat{u}_h), v \rangle_{\partial K_-},$$

that is, that the local residual on K is an extension of the jumps of u_h on ∂K_- , $u_h - \hat{u}_h$, into the element K . This means, roughly speaking, that if the quality of the approximation in the element K is very low, as we expect it would be in the presence of discontinuities, then the local residual, and hence the jumps across the inflow boundary of K , would be huge. This *faux pas* of the method, however, is automatically compensated by an increase in the dissipation of the scheme which results in the effective damping of the typical spurious oscillations that appear around the discontinuities. If, on the other hand, the quality of the approximation in the element is high, as we expect it to be for very smooth solutions, the damping mechanism does not degrade the accuracy of the method since the jumps are properly related to the local residuals. This can be actually rigorously justified, as we see in the next result by Johnson and Pitkäranta (1986).

Theorem 2.1 (Error estimates for the original DG method) *Consider the DG method for the neutron transport equation. Suppose that the approximate solution is a polynomial of degree k on each element K of a locally quasi-uniform grid \mathcal{T}_h . Then we have*

$$\|u - u_h\|_{\Omega} + \Theta_h^{1/2}(u_h) + \left(\sum_{K \in \mathcal{T}_h} h_K \|\mathbf{a} \cdot \nabla(u - u_h)\|_{L^2(K)}^2 \right)^{1/2} \leq C |u|_{H^{k+1}(\Omega)} h^{k+1/2},$$

where C is independent of u and h is the maximum of the diameters of the elements K , h_K .

This rate of convergence was shown to be sharp by Peterson (1991). However, in some instances, the order of convergence of $k+1$ can be obtained. This happens for Cartesian grids and tensor-product polynomials of degree k , see Lesaint and Raviart (1974), and for some structured meshes of triangles and polynomials of degree k , see Richter (1988). For a more detailed discussion on the analysis of the method, see the review by Cockburn et al. (2000).

2.2. Linear, symmetric hyperbolic systems

The original DG method can be readily extended to linear, symmetric hyperbolic systems like the wave equation or the Maxwell equations. To show how to do that, consider the model

Encyclopedia of Computational Mechanics. Edited by Erwin Stein, René de Borst and Thomas J.R. Hughes.

© 2004 John Wiley & Sons, Ltd.

problem

$$\begin{aligned} \mathbf{u}_t + \sum_{i=1}^N A^i \mathbf{u}_{x_i} + B\mathbf{u} &= \mathbf{f}, & \text{in } \Omega \times (0, T), \\ (A\mathbf{n} - M)(\mathbf{u} - \mathbf{u}_D) &= \mathbf{0} & \text{on } \partial\Omega \times [0, T], \\ \mathbf{u}(t=0) &= \mathbf{u}_0 & \text{on } \Omega, \end{aligned}$$

where \mathbf{u} is an \mathbb{R}^m -valued function and A^i is a symmetric matrix for $i = 1, \dots, N$. Here $A\mathbf{n}$ denotes the matrix $\sum_{i=1}^N n_i A^i$ where $\mathbf{n} = (n_1, \dots, n_N)$ is the unit outward normal at the boundary of Ω . Friedrichs (1958) has shown that this problem has a unique solution under some smoothness conditions on the data, under the positivity property

$$B + B^* - \sum_{i=1}^N A_{x_i}^i \geq \beta I, \quad \beta > 0,$$

and under the following properties on the *boundary condition* matrix M :

$$\begin{aligned} M + M^* &\geq 0, \\ \ker(A\mathbf{n} - M) + \ker(A\mathbf{n} + M) &= \mathbb{R}^m & \text{on } \partial\Omega \times [0, T]. \end{aligned}$$

It is very easy to verify that the neutron transport equation is a particular case of the above problem. Indeed, in that case we have that $m = 1$ and so the matrices A^i are real numbers; moreover, we have that $\mathbf{a} = (A^1, \dots, A^N)$ and that $A\mathbf{n} = \mathbf{a} \cdot \mathbf{n}$. The boundary condition matrix M is simply $|\mathbf{a} \cdot \mathbf{n}|$, so that the boundary condition reads

$$(\mathbf{a} \cdot \mathbf{n} - |\mathbf{a} \cdot \mathbf{n}|)(u - u_D) = 0 \quad \text{on } \partial\Omega \times [0, T],$$

that is,

$$u = u_D \quad \text{on } \partial\Omega_- \times [0, T].$$

To define a DG method, we proceed as follows. First, we obtain a mesh \mathcal{T}_h of the space-time domain $\Omega \times (0, T)$. Then, for each element $K \in \mathcal{T}_h$, we take $\mathbf{u}_h|_K$ to be in the finite dimensional space $V(K)$ and define it by requiring that

$$-(\mathbf{u}_h, \mathbf{v}_t)_K - \sum_{i=1}^N (A^i \mathbf{u}_h, \mathbf{v}_{x_i})_K + \left\langle \widehat{A\mathbf{n}_K} \mathbf{u}_h, \mathbf{v} \right\rangle_{\partial K} + \left((B - \sum_{i=1}^N A_{x_i}^i) \mathbf{u}_h, \mathbf{v} \right)_K = (\mathbf{f}, \mathbf{v})_K, \quad (6)$$

for all $\mathbf{v} \in V(K)$. Here we have taken $\widehat{A\mathbf{n}_K} = A\mathbf{n} + n_t Id$, where $\mathbf{n}_K = (\mathbf{n}, n_t)$. Next, let us define the numerical flux $\widehat{A\mathbf{n}_K} \mathbf{u}$.

On the border of the space-time domain, we take

$$\widehat{A\mathbf{n}_K} \mathbf{u}_h = \begin{cases} \mathbf{u}_0 & \text{on } \Omega \times \{t = 0\}, \\ \mathbf{u}_h & \text{on } \Omega \times \{t = T\}, \\ \frac{1}{2} A\mathbf{n}(\mathbf{u}_h + \mathbf{u}_D) + \frac{1}{2} M(\mathbf{u}_h - \mathbf{u}_D) & \text{on } \partial\Omega \times (0, T), \end{cases}$$

and on the inter-element boundaries,

$$\widehat{A\mathbf{n}_K} \mathbf{u}_h = \widehat{A\mathbf{n}_K} \{\mathbf{u}_h\} + \frac{1}{2} \mathbb{M} \llbracket \mathbf{u}_h \rrbracket \mathbf{n}_K,$$

where

$$\{\mathbf{u}_h\} = \frac{1}{2}(\mathbf{u}_h^- + \mathbf{u}_h^+), \quad \text{and} \quad \llbracket \mathbf{u}_h \rrbracket_{\mathbf{n}_K} = \mathbf{u}_h^- - \mathbf{u}_h^+ \quad \text{where} \quad \mathbf{u}_h^\pm(\mathbf{x}) = \lim_{\epsilon \downarrow 0} \mathbf{u}_h(\mathbf{x} \pm \epsilon \mathbf{n}_K).$$

It only remains to define the matrices \mathbb{M} . The two main choices are $\mathbb{M} = |\mathbb{A}_{\mathbf{n}_K}|$, which gives rise to the so-called upwinding numerical flux, and $\mathbb{M} = \rho(\mathbb{A}_{\mathbf{n}_K}) Id$, where $\rho(E)$ is the spectral radius of the matrix E , which gives rise to the so-called Lax-Friedrichs numerical flux. This completes the definition of the DG method.

Note how the numerical flux has three key properties: (i) it only depends on the traces of the approximation on the boundary of the elements, (ii) it is consistent and, (iii) it is conservative. Let us discuss these properties. The first renders the numerical fluxes easy to evaluate and ensures a high degree of locality of the method.

The property of consistency ensures that we are approximating the correct exact solution. It is satisfied if

$$\widehat{\mathbb{A}_{\mathbf{n}_K} \mathbf{u}} = \mathbb{A}_{\mathbf{n}_K} \mathbf{u},$$

where \mathbf{u} is the exact solution. Since $\llbracket \mathbf{u} \rrbracket_{\mathbf{n}_K} = \mathbf{0}$, we do have that the numerical flux is consistent in the inter-element boundaries. It is trivial to see it is consistent on $\Omega \times \{t = 0\}$ and on $\Omega \times \{t = T\}$. It remains to see what happens on $\partial\Omega \times (0, T)$. But we have

$$\widehat{\mathbb{A}_{\mathbf{n}_K} \mathbf{u}} = \frac{1}{2} \mathbb{A}_{\mathbf{n}}(\mathbf{u} + \mathbf{u}_D) + \frac{1}{2} M(\mathbf{u} - \mathbf{u}_D) = \mathbb{A}_{\mathbf{n}} \mathbf{u} + \frac{1}{2} (M - \mathbb{A}_{\mathbf{n}})(\mathbf{u} - \mathbf{u}_D) = \mathbb{A}_{\mathbf{n}} \mathbf{u},$$

since the exact solution satisfies the boundary condition $(M - \mathbb{A}_{\mathbf{n}})(\mathbf{u} - \mathbf{u}_D) = 0$. The numerical flux is thus consistent.

Conservativity is a property of the numerical flux in the inter-element boundaries that ensures that the convective properties of the exact solution are properly captured. It is satisfied if

$$\widehat{\mathbb{A}_{\mathbf{n}_{K_1}} \mathbf{u}_h} + \widehat{\mathbb{A}_{\mathbf{n}_{K_2}} \mathbf{u}_h} = \mathbf{0},$$

on the intersection of the boundaries of the elements K_1 and K_2 . A glance to the definition of the numerical fluxes will convince the reader that the numerical fluxes are indeed conservative. As a consequence, for any set S which is the union of elements $K \in \mathcal{T}_h$, we have

$$\int_S \left(B - \sum_{i=1}^N A_{x_i}^i \right) \mathbf{u}_h dx + \int_{\partial S} \widehat{\mathbb{A}_{\mathbf{n}_S} \mathbf{u}_h} ds = \int_S \mathbf{f} dx.$$

Next, let us address the issue of how to actually solve for the approximate solution. For general numerical fluxes and general meshes, the above DG method gives rise to a matrix equation involving all the degrees of freedom of the approximate solution. However, if the upwinding flux is used on $\Omega \times \{t^n\}$ and on $\Omega \times \{t^{n+1}\}$, it is possible to solve only on the time slab $\Omega \times [t^n, t^{n+1}]$, as proposed by Johnson et al. (1984). Unfortunately, this gives rise to globally implicit method; see Fig. 2 (left). This difficulty can be avoided if *suitably* defined meshes are used together with the *upwinding* numerical flux as shown by Lowrie et al. (1995), Lowrie (1996), Lowrie et al. (1998) in the frame of non-linear hyperbolic systems, and later by Yin et al. (2000) in the framework of elastodynamics, and by Falk and Richter (1999) in the framework of linear symmetric hyperbolic systems. See Fig. 2 (right).

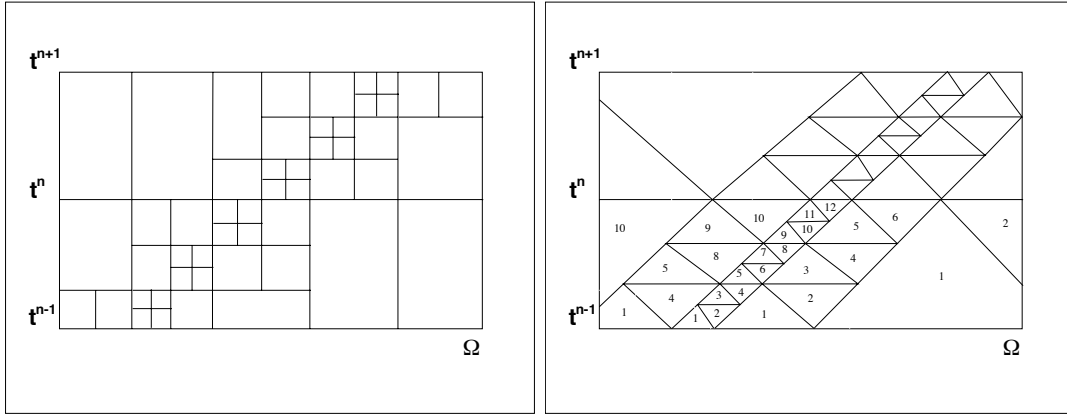


Figure 2. Space-time meshes for the DG method. On each time slab $\Omega \times (t^m, t^{m+1})$, the resolution can be globally implicit (left) or implicit only on each element (right).

Concerning the stability of the DG method, we can say that, just as for the original DG method, the stability of the DG method for linear, symmetric systems is enhanced by the jumps of the approximate solution. Indeed, a simple computation gives

$$J(\mathbf{u}) = L(\mathbf{u}),$$

where \mathbf{u} is the exact solution and

$$J(\mathbf{u}) = (\sigma \mathbf{u}, \mathbf{u})_{\Omega \times (0, T)} + \frac{1}{2} \langle 1, \mathbf{u}^2 \rangle_{\Omega \times \{t=0\}} + \frac{1}{2} \langle 1, \mathbf{u}^2 \rangle_{\Omega \times \{t=T\}} + \frac{1}{2} \langle M \mathbf{u}, \mathbf{u} \rangle_{\partial \Omega \times [0, T]},$$

and

$$L(\mathbf{u}) = (\mathbf{f}, \mathbf{u})_{\Omega \times (0, T)} + \langle \mathbf{u}, \mathbf{u}_0 \rangle_{\Omega \times \{t=0\}} + \frac{1}{2} \langle (M - A \mathbf{n}) \mathbf{u}_D, \mathbf{u} \rangle_{\partial \Omega \times [0, T]}.$$

From the above equality, we can obtain an a priori estimate on the exact solution. A similar computation for the DG method gives

$$J(\mathbf{u}_h) + \Theta_h(\mathbf{u}_h) = L(\mathbf{u}_h),$$

where

$$\Theta_h(\mathbf{u}_h) = \frac{1}{2} \sum_{e \in \mathcal{E}_h^i} \langle \mathbb{M} [\mathbf{u}_h] \mathbf{n}_e, [\mathbf{u}_h] \mathbf{n}_e \rangle_e.$$

Here \mathcal{E}_h^i is the set of inter-element boundaries and \mathbf{n}_e any of the two normals to e . We thus see, once more, that the stability of the method is enhanced through the jumps of the approximate solution. We also see that the role of the matrix \mathbb{M} is to control the amount and type of dissipation of the scheme. Indeed, if $\mathbb{M} = 0$, the DG method would not have dissipation at all. Moreover, if we take the Lax-Friedrichs numerical scheme, the dissipation is isotropic whereas if we take the upwinding scheme, anisotropic.

Let us end our discussion of the extension of the original DG method to linear, symmetric systems by briefly stating that there is also a linear relationship between the local residual

and the jumps of the approximate solution. Moreover, the error estimate for the original DG method can be proven to be of order $k+1/2$ for suitably defined grids and for smooth solutions when polynomials of degree k are used. For details, see the work of Johnson et al. (1984) and that of Falk and Richter (1999).

The method of lines for these systems has been studied by Cockburn et al. (2003) where it was shown that, if uniform grids are used, a local post-processing of the approximate solution of the DG method is of order $2k+1$ when polynomials of degree k are used. These results can be easily extended to the DG methods under consideration. Let us illustrate this phenomenon on the model problem,

$$u_t + u_x = 0, \quad \text{in } (0, 2\pi) \times (0, T) \quad u(x, 0) = \sin(x) \quad x \in (0, 2\pi), \quad (7)$$

with periodic boundary conditions. In Table 2.2, we see that the order of convergence of both the L^2 and L^∞ errors for P^k elements is of $(k+1)$ before post-processing and of at least $(2k+1)$ after post-processing, for $k=1, 2, 3, 4$. In Fig. 3, we see the absolute errors before and after post-processing for P^2 . The post-processing of the approximate solution is obtained by convolution with a kernel whose support is the union of a number of elements which only depends on k ; for details, see Cockburn et al. (2003).

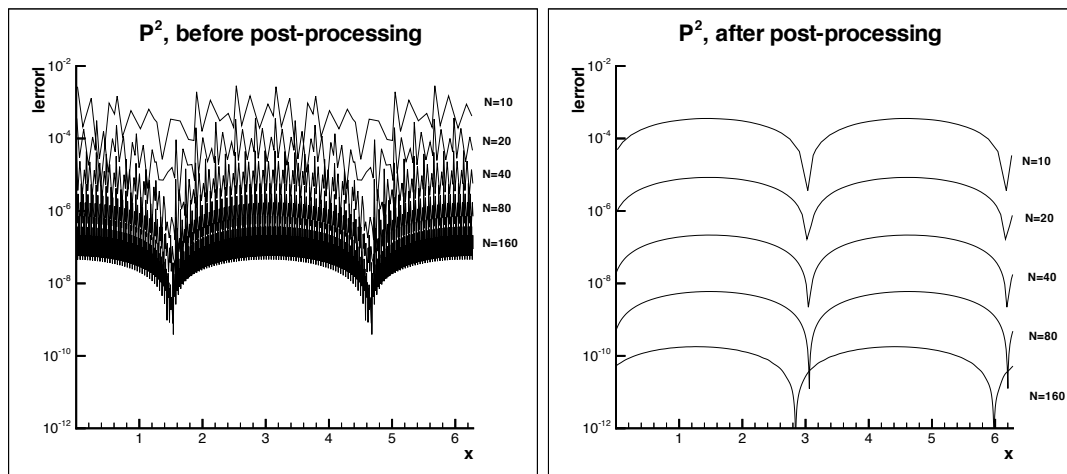


Figure 3. The absolute value of the errors for P^2 with $N=10, 20, 40, 80$ and 160 elements. Before post-processing (left) and after post-processing (right). From Cockburn et al. (2003).

3. Non-linear hyperbolic problems

In this section, we consider DG methods for non-linear hyperbolic problems. We begin by showing that to ensure convergence towards the physically relevant solution, usually called the *entropy solution*, the DG methods need to use a numerical flux based on a suitable *approximate Riemann solver* and that they must use either a *shock-capturing* term or a *slope limiter*. We show that the shock-capturing DG methods are strongly related to stabilized

Table I. The effect of post-processing the approximate solution. From Cockburn et al. (2003).

mesh	Before postprocessing				After postprocessing			
	L^2 error	order	L^∞ error	order	L^2 error	order	L^∞ error	order
P^1								
10	3.29E-02	—	5.81E-02	—	3.01E-02	—	4.22E-02	—
20	5.63E-03	2.55	1.06E-02	2.45	3.84E-03	2.97	5.44E-03	2.96
40	1.16E-03	2.28	2.89E-03	1.88	4.79E-04	3.00	6.78E-04	3.01
80	2.72E-04	2.09	8.08E-04	1.84	5.97E-05	3.00	8.45E-05	3.00
160	6.68E-05	2.03	2.13E-04	1.93	7.45E-06	3.00	1.05E-05	3.00
320	1.66E-05	2.01	5.45E-05	1.96	9.30E-07	3.00	1.32E-06	3.00
P^2								
10	8.63E-04	—	2.86E-03	—	2.52E-04	—	3.57E-04	—
20	1.07E-04	3.01	3.69E-04	2.95	5.96E-06	5.40	8.41E-06	5.41
40	1.34E-05	3.00	4.63E-05	3.00	1.53E-07	5.29	2.16E-07	5.28
80	1.67E-06	3.00	5.78E-06	3.00	4.22E-09	5.18	5.97E-09	5.18
160	2.09E-07	3.00	7.23E-07	3.00	1.27E-10	5.06	1.80E-10	5.06
P^3								
10	3.30E-05	—	9.59E-05	—	1.64E-05	—	2.31E-05	—
20	2.06E-06	4.00	6.07E-06	3.98	7.07E-08	7.85	1.00E-07	7.85
40	1.29E-07	4.00	3.80E-07	4.00	2.91E-10	7.92	4.15E-10	7.91
50	5.29E-08	4.00	1.56E-07	4.00	5.03E-11	7.87	7.24E-11	7.83
P^4								
10	1.02E-06	—	2.30E-06	—	1.98E-06	—	2.81E-06	—
20	3.21E-08	5.00	7.30E-08	4.98	2.20E-09	9.82	3.11E-09	9.82
30	4.23E-09	5.00	9.66E-09	4.99	4.34E-11	9.68	6.66E-11	9.48

methods like the streamline diffusion method, and that slope-limiter DG methods can be considered to be an extension of finite volume methods. We then show computational results for some shock-capturing DG methods and describe and analyze the so-called Runge-Kutta DG (RKDG) method, a slope-limiter DG method. We show how the different ingredients of the method, namely, the DG space discretization, a special Runge-Kutta time discretization, and a *generalized* slope limiter, are put together to ensure its stability. Finally, several numerical experiments showing the performance of the RKDG methods are given. Particular attention is devoted to the Euler equations of gas dynamics.

3.1. The main difficulty: The loss of well-posedness

Devising numerical methods for non-linear hyperbolic problems is dramatically different from devising methods for linear symmetric hyperbolic problems. This is due to the fact that whereas linear, symmetric hyperbolic problems are well posed, non-linear hyperbolic problems are not.

This difficulty was uncovered first in the framework of the Euler equations of gas dynamics; indeed, this equation has several non-physical *weak* solutions. This happens because the

Euler equations of gas dynamics are obtained from the compressible Navier-Stokes by simply dropping from the equations the terms modeling viscosity and heat transfer effects. As a consequence, the information concerning the second law of thermodynamics is completely lost and discontinuous solutions which violate a such law suddenly appear. To devise numerical schemes that are guaranteed to converge to the entropy solution and not to any other weak solution constitutes the main difficulty of devising numerical methods for non-linear hyperbolic problems.

This difficulty is present even in the simplest hyperbolic problem, namely, the scalar hyperbolic conservation law

$$\begin{aligned} u_t + (f(u))_x &= 0 && \text{in } (0, 1) \times (0, T), \\ u(t = 0) &= u_0 && \text{on } (0, 1), \end{aligned}$$

with periodic boundary conditions. To illustrate this phenomenon, consider the well known Engquist-Osher and Lax-Wendroff schemes and let us apply them to the above equation for $f(u) = u^2/2$ and $u_0(x) = 1$ on $(.4, .6)$ and $u_0(x) = 0$ otherwise. In the Fig. 4, we see that the approximation given by the Engquist-Osher scheme converges to the entropy solution whereas that given by the Lax-Wendroff scheme does not. The Lax-Wendroff scheme lacks a mechanism that ensures its convergence towards the entropy solution and, as a consequence, can converge to a weak solution which is not the entropy solution.

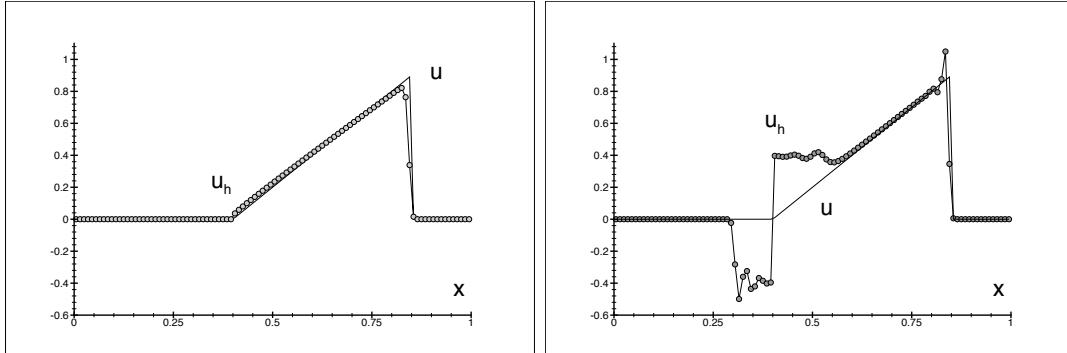


Figure 4. The entropy solution, u , and its approximation u_h at time $T = 1/2$: Engquist–Osher scheme (left) and Lax–Wendroff scheme (right). From Cockburn (2003a).

3.2. Tools for capturing the entropy solution: Heuristics

The DG methods try to ensure convergence towards the entropy solution by using the so-called *Riemann solvers* and either a *shock-capturing term* or a *slope limiter*. To describe the heuristics behind their construction, we consider the parabolic problem

$$\begin{aligned} u_t + (f(u))_x &= \nu u_{xx} && \text{in } (0, 1) \times (0, T), \\ u(t = 0) &= u_0 && \text{on } (0, 1), \end{aligned}$$

since it is known that as the viscosity coefficient ν goes to zero, the solution of the above problem converges to the entropy solution of our scalar hyperbolic conservation law.

Given this property, our strategy is to use the weak formulation of the parabolic problem to see what are the tools that should be used to devise DG methods that converge to the entropy solution. Thus, multiplying the parabolic equation by a test function φ , and integrating over the space-time element K , we get

$$\int_{\partial K} (f(u) - \nu u_x, u) \cdot (n_x, n_t) \varphi ds - \int_K (f(u) - \nu u_x, u) \cdot (\varphi_x, \varphi_t) dx dt = 0.$$

Now, if we set $F\mathbf{n}_K(u) = (f(u) - \nu u_x, u) \cdot (n_x, n_t)$, on ∂K , we end up with

$$\int_{\partial K} F\mathbf{n}_K(u) \varphi ds - \int_K (f(u), u) \cdot (\varphi_x, \varphi_t) + \int_K \nu u_x \varphi_x dx dt = 0.$$

Finally, noting that we have

$$\nu u_x(x, t) = \int_{x(t)}^x R(u)(y, t) dy.$$

where $R(u) = u_t + (f(u))_x$ and $x(t)$ is such that $u_x(x(t), t) = 0$ (such a point always exists because we have periodic boundary conditions), this suggests the so-called shock-capturing DG methods:

$$\int_{\partial K} \widehat{F}\mathbf{n}_K(u_h) \varphi ds - \int_K (f(u_h), u_h) \cdot (\varphi_x, \varphi_t) + \int_K \widehat{\nu} (u_h)_x \varphi_x dx dt = 0,$$

where $\widehat{F}\mathbf{n}_K(u_h)$ is the approximate Riemann solver and the last term is the shock-capturing term.

The approximate Riemann solver is nothing but a numerical trace for the function $F\mathbf{n}_K(u)$; it only depends on the two traces of the function u , that is, $\widehat{F}\mathbf{n}_K(u_h) = \widehat{g}(u_h^-, u_h^+)$. The main examples are the following:

(i) The Godunov flux:

$$\widehat{g}^G(a, b) = \begin{cases} \min_{a \leq u \leq b} g(u), & \text{if } a \leq b, \\ \max_{b \leq u \leq a} g(u), & \text{otherwise.} \end{cases}$$

(ii) The Engquist-Osher flux:

$$\widehat{g}^{EO}(a, b) = \int_0^b \min(g'(s), 0) ds + \int_0^a \max(g'(s), 0) ds + g(0);$$

(iii) The Lax-Friedrichs flux:

$$\widehat{g}^{LF}(a, b) = \frac{1}{2} [g(a) + g(b) - C(b - a)], \quad C = \max_{\inf u^0(x) \leq s \leq \sup u^0(x)} |g'(s)|.$$

The shock-capturing term has the same structure than the corresponding term for the parabolic equation and typically has a viscosity coefficient $\widehat{\nu}$ that depends on the residual as follows:

$$\widehat{\nu} = \delta^\alpha \frac{|R(u_h)|}{|(u_h)_x| + \epsilon},$$

where the auxiliary parameter δ is usually taken to be of the order of the diameter of K and α is a parameter usually bigger than one and smaller than 2. The purpose of the small number ϵ is to prevent a division by zero when $(u_h)_x = 0$. The shock-capturing DG methods considered by Jaffré et al. (1995) and by Cockburn and Gremaud (1996) for the scalar hyperbolic conservation law in several space dimensions are of this form.

The DG methods that do not have a shock-capturing term *must* have a slope limiter in order to ensure that the information about the entropy solution is incorporated into the scheme. In fact, as we argue next, the slope limiters and the shock-capturing terms have exactly the same origin. The DG methods with a slope limiter are obtained as follows. Instead of keeping the shock-capturing term in a single equation, that term is *split-off* in a way typical of operator splitting techniques. Take $K = I \times (t^n, t^{n+1})$. To march from time t^n to t^{n+1} , we first compute $u_h^{n+1/2}$ from u_h^n by using the scheme

$$\int_{\partial K} (\widehat{f}_h, \widehat{u}_h) \cdot (n_x, n_t) \varphi ds - \int_K (f(u_h), u_h) \cdot (\varphi_x, \varphi_t) dx dt = 0,$$

for some numerical flux $(\widehat{f}_h, \widehat{u}_h) \cdot (n_x, n_t)$, and then, compute u_h^{n+1} from $u_h^{n+1/2}$ by using

$$\int_I (u_h^{n+1} - u_h^{n+1/2}) \varphi dx - (t^{n+1} - t^n) \int_I \nu (u_h^{n+1/2})_x \varphi_x dx = 0.$$

We thus see that the function u_h^{n+1} captures the information contained in the shock-capturing term. The link between this second step and the so-called slope limiters can be easily established if we realize that, if we write,

$$u_h^{n+1} = \Lambda \Pi_h u_h^{n+1/2},$$

then, the operator $\Lambda \Pi_h$ is actually a (generalized) slope limiter.

Let us illustrate this fact on a simple case. Consider the piecewise linear function v_h and set $u_h = \Lambda \Pi(v_h)$, that is, u_h is the piecewise linear function defined by

$$\int_I u_h \varphi dx = \int_I v_h \varphi dx - \int_I \text{slc} (v_h)_x \varphi_x dx,$$

where $\text{slc} := (t^{n+1} - t^n) \nu$, for all linear functions φ . If we write

$$v_h(x) = \bar{v}_j + (x - x_j) v_{x,j},$$

on each interval I_j , and take

$$\text{slc} = \begin{cases} 0 & \text{if } v_{x,j} = 0, \\ \frac{h_j^2}{12} \left(1 - m \left(1, \frac{2}{h_j} \frac{\bar{v}_j - \bar{v}_{j-1}}{v_{x,j}}, \frac{2}{h_j} \frac{\bar{v}_{j+1} - \bar{v}_j}{v_{x,j}} \right) \right) & \text{otherwise,} \end{cases}$$

where the *minmod* function m is defined by

$$m(a_1, a_2, a_3) = \begin{cases} s \min_{1 \leq n \leq 3} |a_n| & \text{if } s = \text{sign}(a_1) = \text{sign}(a_2) = \text{sign}(a_3), \\ 0 & \text{otherwise,} \end{cases}$$

we obtain that

$$\bar{u}_j = \bar{v}_j, \quad \text{and} \quad u_{x,j} = m(v_{x,j}, \bar{v}_j - \bar{v}_{j-1}, \bar{v}_{j+1} - \bar{v}_j)$$

We thus see that the mean of u_h coincides with that of v_h . Moreover, since, by definition of the function m , we have

$$|u_{x,j}| \leq |v_{x,j}|,$$

it is reasonable to call the operator Π a slope limiter. This slope limiter is due to Osher (1984); see Fig. 5. It is less restrictive than the limiters originally considered by van Leer (1974) and by van Leer (1979).

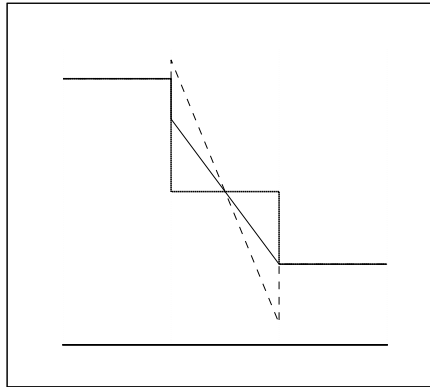


Figure 5. The Π_h^O limiter: An example. Displayed are the local means of u_h (thick line), the linear function u_h in the element of the middle before limiting (dotted line) and the resulting function after limiting (solid line).

Next, we show computational results for some shock-capturing DG methods and then study the main example of DG methods using slope limiters, namely, the Runge-Kutta discontinuous Galerkin (RKDG) methods.

3.3. Shock-capturing DG methods

There are only two theoretical results concerning shock-capturing methods, and those concern the scalar hyperbolic conservation law. The first is by Jaffré et al. (1995), who proved convergence to the entropy solution. The second is by Cockburn and Gremaud (1996), who showed that this convergence takes place at rate of at least $h^{1/4}$ in the $L^\infty(0, T; L^1(\mathbb{R}^N))$ -norm; a posteriori error estimates were also proven which have not yet been exploited for adaptivity purposes.

Space-time DG methods for non-linear hyperbolic conservation laws were considered by Lowrie et al. (1995), Lowrie (1996) and Lowrie et al. (1998). More recently, DG shock-capturing methods have been considered by Hartmann and Houston (2002a) and Hartmann and Houston (2002b) for adaptively solving for values of linear functionals of solutions of *steady state* non-linear hyperbolic conservation laws with remarkable success; see also Süli and Houston (2002).

To give an example, let us consider the Burger's equation

$$u_t + \frac{1}{2} (u^2)_x = 0, \quad \text{in } \Omega \times (0, T),$$

where $\Omega = (0, 3)$ and $T = 2$, subject to the initial condition

$$u(x, 0) = \begin{cases} 2 \sin^2(\pi x), & 0 \leq x \leq 1, \\ \sin^2(\pi x), & 1 \leq x \leq 2, \\ 0, & 2 \leq x \leq 3, \end{cases}$$

and boundary condition $u(0, t) = 0$, for $t \in [0, T]$; see Fig. 6. The exact solution develops two shocks which eventually merge. The functional of interest $J(\cdot)$ is the value of the solution before these two shocks collapse into each other. We thus take,

$$J(u) = u(2.3, 1.5) = 0.664442403975254670;$$

see Fig. 6.

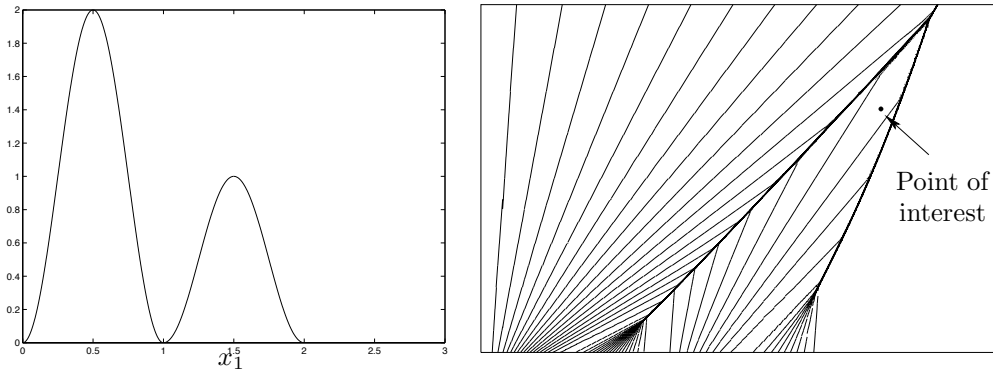


Figure 6. Burgers' problem: Initial condition (left) and isolines for the exact solution (right). From Süli and Houston (2002)

In Fig. 7, we compare the performance of the h - and hp -mesh refinement algorithms for this problem. Again, we observe exponential convergence of the error in the computed functional using hp -refinement; on the linear-log scale, the convergence line is straight. On the final mesh the true error between $J(u)$ and $J(u_{\text{DG}})$ using hp -refinement is almost 5 orders of magnitude smaller than the corresponding quantity when h -refinement is employed alone. Furthermore, in Fig. 7, we observe that the hp -refinement algorithm also outperforms the h -refinement strategy, when comparing the error in the computed target functional with respect to the computational cost. Indeed, Fig. 8 clearly shows that for the hp -DGFEM the cost per degree of freedom when hp -refinement is employed is comparable to that of using h -refinement.

Finally, in Fig. 9 we show the primal mesh after 11 adaptive hp -mesh refinements. Here, we see that the h -mesh has been refined in the region upstream of the point of interest, thereby isolating the smooth region of u from the two interacting shock waves; this renders the subsequent p -refinement in this region much more effective.

Now, let us consider the problem of computing the drag coefficient, $J(\mathbf{u})$, of the NACA0012 airfoil for two flows. The first is sub-sonic and is obtained by imposing on the outer boundary a Mach 0.5 flow at a zero angle of attack, and a far-field density $\rho = 1$ and pressure $p = 1$. In this case, no shock-capturing term is used since the solution is very smooth. The second flow is

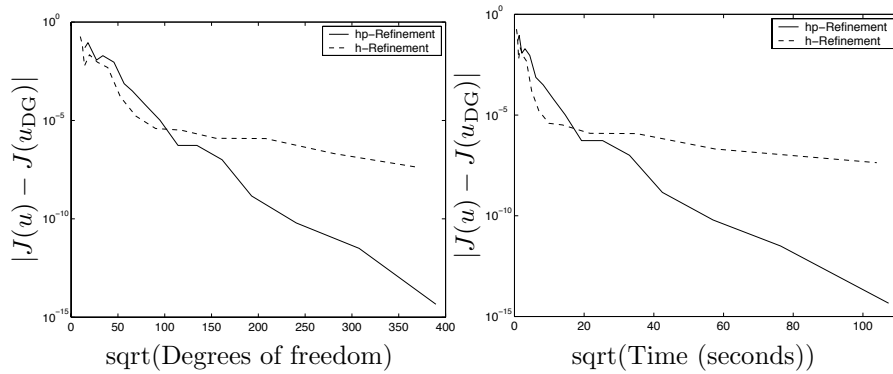


Figure 7. Burgers' equation. Comparison between h - and hp -adaptive mesh refinement: $|J(u) - J(u_{DG})|$ versus number of degrees of freedom (left); $|J(u) - J(u_{DG})|$ versus computational time (right). From Süli and Houston (2002)

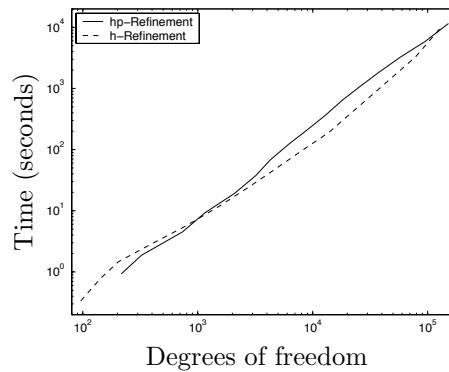


Figure 8. Burgers' equation. Computational time versus number of degrees of freedom

obtained by imposing this time a Mach 0.8 flow and an angle of attack $\alpha = 1.25^\circ$. Since in this case, the solution presents a shock, the shock-capturing term is turned on. In Fig. 10, we see how easily the DG method handles meshes with hanging nodes and with different polynomials degrees in different elements. In Fig. 11, we also see that hp -adaptivity is more efficient than h -adaptivity even in the presence of shocks.

Also recently, van der Vegt and van der Ven (2002b) (see also the paper by van der Ven and van der Vegt (2002)) have considered shock-capturing DG methods for the time-dependent compressible Euler equations of gas dynamics. Accordingly, they have used space-time elements, which allow them to easily deal with moving bodies. Their shock-capturing term uses both the local residuals as well as the jumps which, as we have seen, are also related to the local residuals; for details, see van der Vegt and van der Ven (2002b). They have shown that this method can be efficiently used with mesh adaptation. As an example, we show in Fig. 12, the approximation of the method with mesh adaptation on a time-dependent Mach 0.8 flow around an oscillating NACA 0012 airfoil. The pitching angle is between -0.5° and

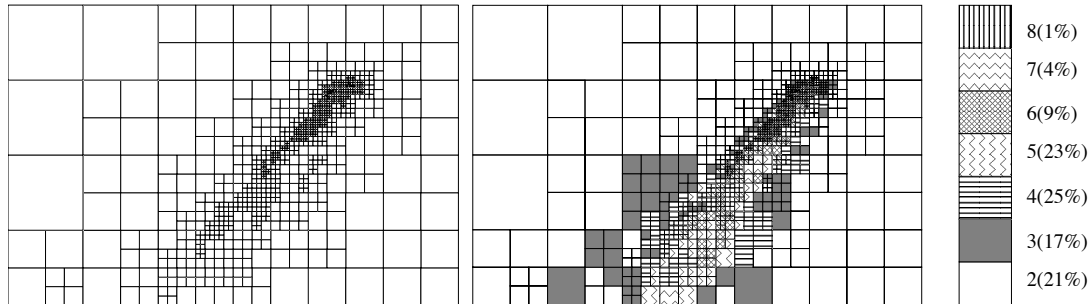


Figure 9. Burgers' equation. h - and hp -meshes after 11 refinements, with 999 elements and 26020 degrees of freedom; here, $|J(u) - J(u_{\text{DG}})| = 1.010 \times 10^{-7}$. From Süli and Houston (2002)

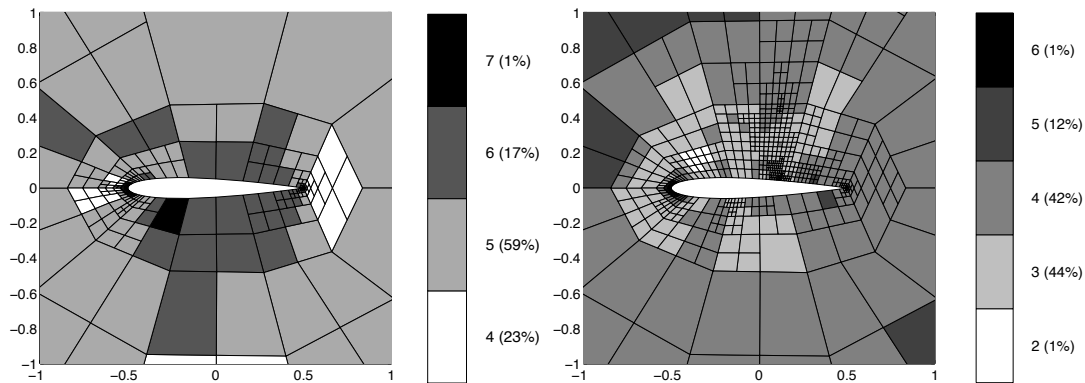


Figure 10. Flow around a NACA0012 airfoil: Sub-sonic (left) and supersonic (right). The actual hp -meshes after 10 refinements. For the sub-sonic flow, the hp -mesh has 325 elements, 45008 degrees of freedom, and produces an error $|J(\mathbf{u}) - J(\mathbf{u}_h)| = 3.756 \times 10^{-7}$. For the transonic flow, it has 783 elements, 69956 degrees of freedom, and produces an error of $|J(\mathbf{u}) - J(\mathbf{u}_{\text{DG}})| = 1.311 \times 10^{-4}$. From Süli and Houston (2002).

4.5° , and the circular frequency is $\omega = \pi/10$. A more spectacular example is shown in Figs. 13, 14 and 15, where their DG method is applied to helicopter flight.

3.4. The RKDG methods

There are two main differences between the RKDG methods and the shock-capturing DG methods. The first is that the RKDG methods use an explicit Runge-Kutta scheme to evolve the approximate solution in time; this renders them very easy to implement and much more parallelizable. The second is that whereas the shock-capturing DG methods converge to the entropy solution thanks to the inclusion in their weak formulation of the shock-capturing terms, the RKDG achieve this by using a slope limiters. Although these two techniques have the very same origin, as we showed in the previous subsection, the use of the slope limiters

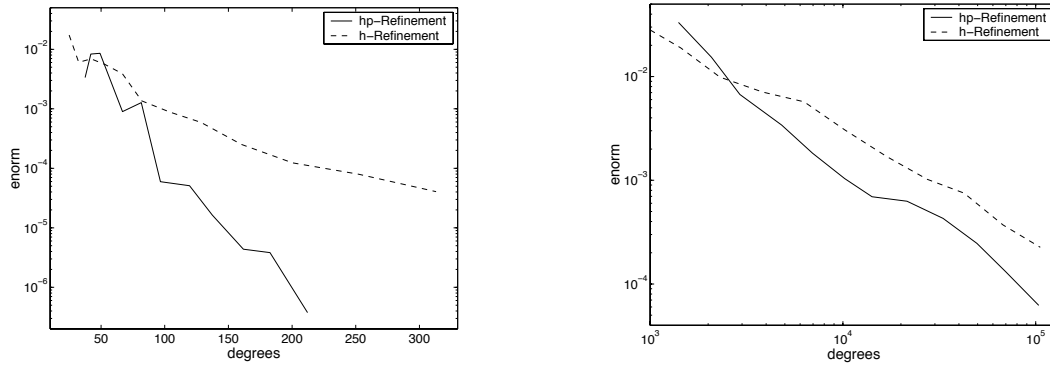


Figure 11. Flow around a NACA0012 airfoil: Sub-sonic (left) and supersonic (right). Comparison between h - and hp -adaptive mesh refinement. From Süli and Houston (2002).

results in sharper approximations to the shocks and contact discontinuities.

In this subsection, we consider the Runge-Kutta discontinuous Galerkin (RKDG) methods for non-linear hyperbolic systems in divergence form,

$$\mathbf{u}_t + \sum_{i=1}^N (\mathbf{f}_i(\mathbf{u}))_{x_i} = \mathbf{0}.$$

To define the RKDG methods, we proceed in three steps. In the first, the conservation law is discretized in space by using a discontinuous Galerkin (DG) method. After discretization, the system of ordinary differential equations $\frac{d}{dt}\mathbf{u}_h = \mathbf{L}(\mathbf{u}_h)$ is obtained. Since the approximation is discontinuous, the so-called *mass matrix* is block diagonal and hence, easily invertible. In the second step, an *explicit* strong stability preserving (SSP) Runge-Kutta method is used to march in time. The distinctive feature of the SSP-RK methods is that their stability follows from the stability of the forward Euler step. Finally, in the third step, a *generalized slope limiter* $\Lambda\Pi_h$, is introduced in order to *enforce* the above mentioned stability property of the Euler forward step.

In what follows, we give a detailed construction of the RKDG method for the model problem of the scalar conservation law in one space dimension. Then, we briefly discuss the extension of the method to hyperbolic systems in several space dimensions and present numerical results showing the performance of the method.

3.5. RKDG methods for scalar hyperbolic non-linear conservation laws

Let us define the RKDG method for the Cauchy problem for the scalar hyperbolic non-linear conservation law

$$u_t + f(u)_x = 0, \quad \text{in } (0, 1) \times (0, T), \quad u(x, 0) = u_0(x), \quad \forall x \in (0, 1), \quad (8)$$

with periodic boundary conditions.

3.5.1. The DG space discretization Let us triangulate the domain $[0, 1)$ with the partition $\mathcal{T}_h = \{I_j\}_{j=1}^N$ where $I_j = (x_{j-1/2}, x_{j+1/2})$. The initial data $u_h(\cdot, 0)|_{I_j}$ is simply the L^2 -

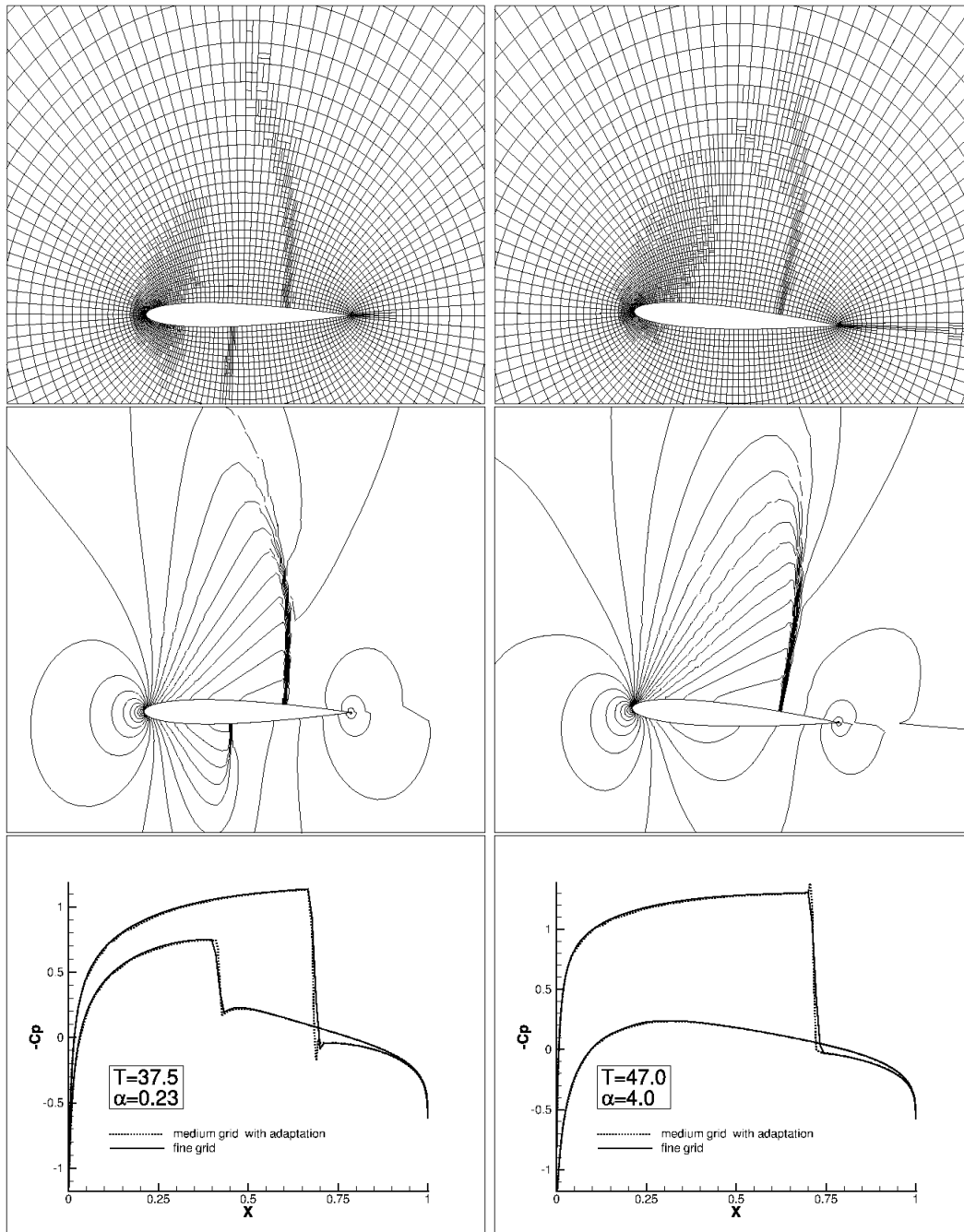


Figure 12. Adapted mesh around oscillating NACA 0012 airfoil, contours of density, and pressure coefficient C_p on the airfoil surface for $\alpha = 0.23^\circ$ (pitching upward) and $\alpha = 4.0^\circ$ (pitching downward) ($M_\infty = 0.8$, $\omega = \pi/10$, $\alpha = 2^\circ \pm 2.5^\circ$). From van der Vegt and van der Ven (2002b).

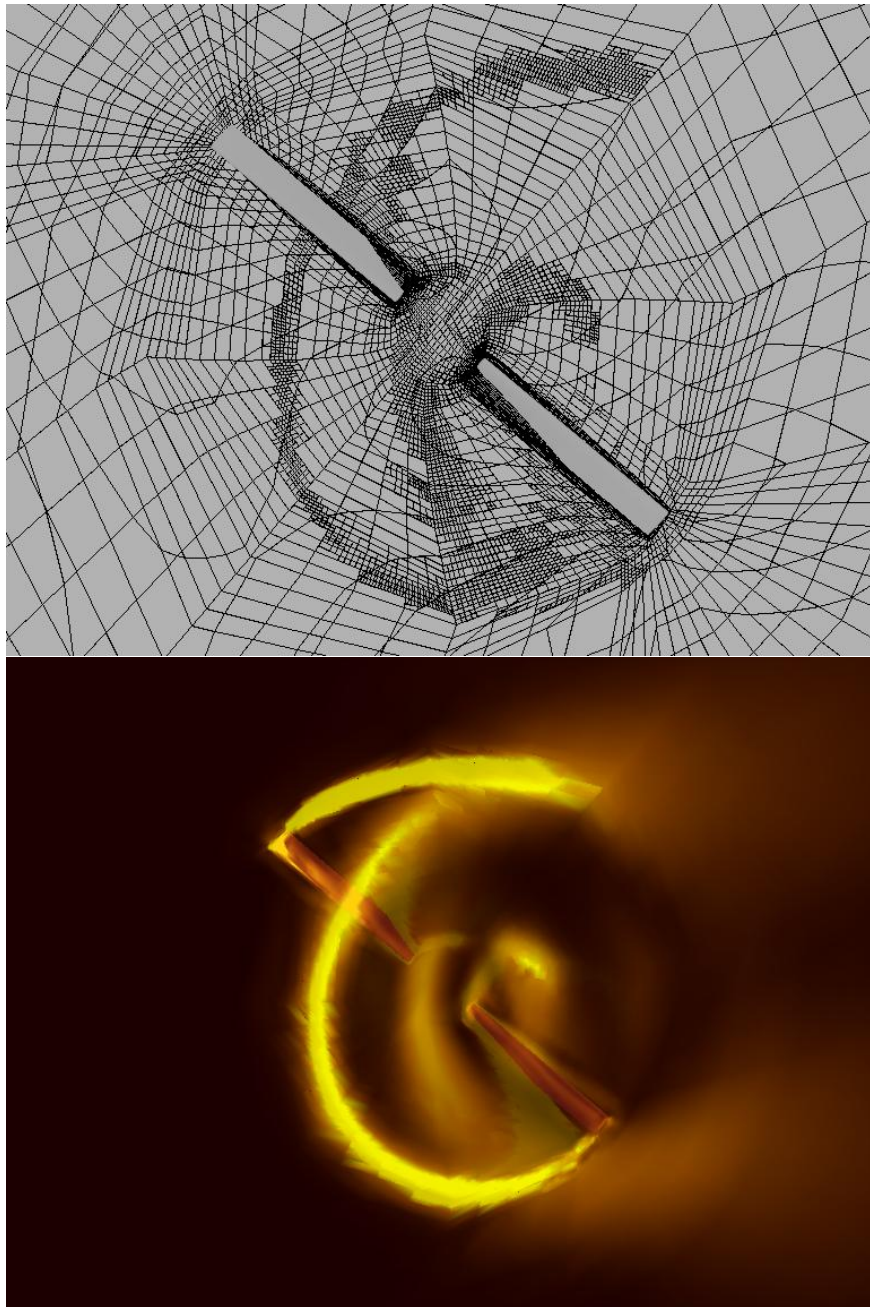


Figure 13. Four-dimensional simulation of the Operational Loads Survey rotor in forward flight. Grid cross-section at $z = 0$ (top) and vorticity levels (bottom) on adapted grid at azimuth $\psi = 140^\circ$. The tip vortex of the blade in the upper corner lies above the $z = 0$ plane. ($M_{\text{tip}} = 0.664$, advance ratio 0.164, and thrust 0.0054, flow is coming from the left). From van der Ven and Boelens (2003).

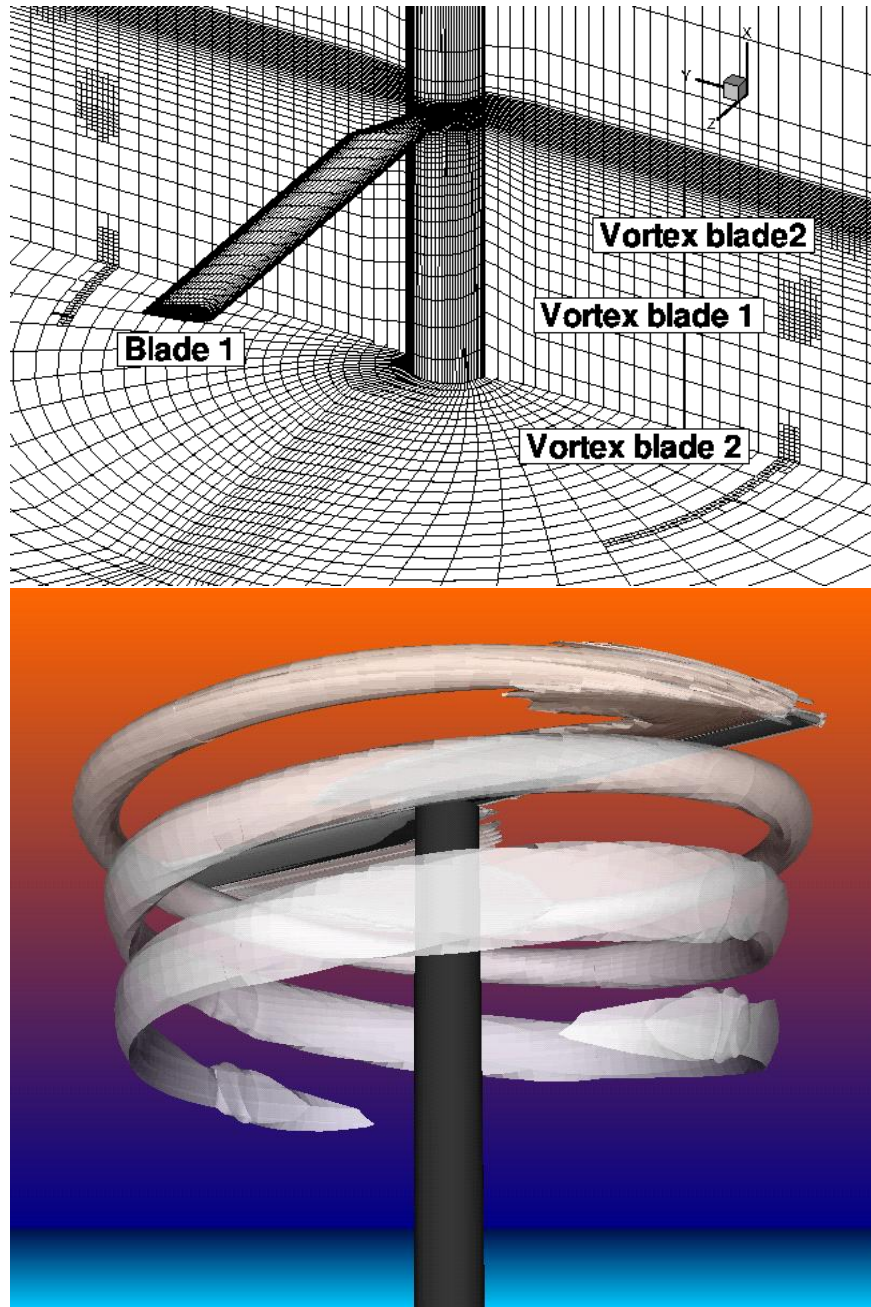


Figure 14. Adapted Caradonna-Tung rotor grid (135.280 elements) with periodic plane at $z = 0$ and horizontal plane at $x = -3.6$, showing the refined regions at the vortex locations (top). Vorticity contours ($|\omega| = 0.175$) for the Caradonna-Tung rotor in hover, collective pitch 12° , and $M_{\text{tip}} = 0.61$ (bottom). From Boelens et al. (2002)

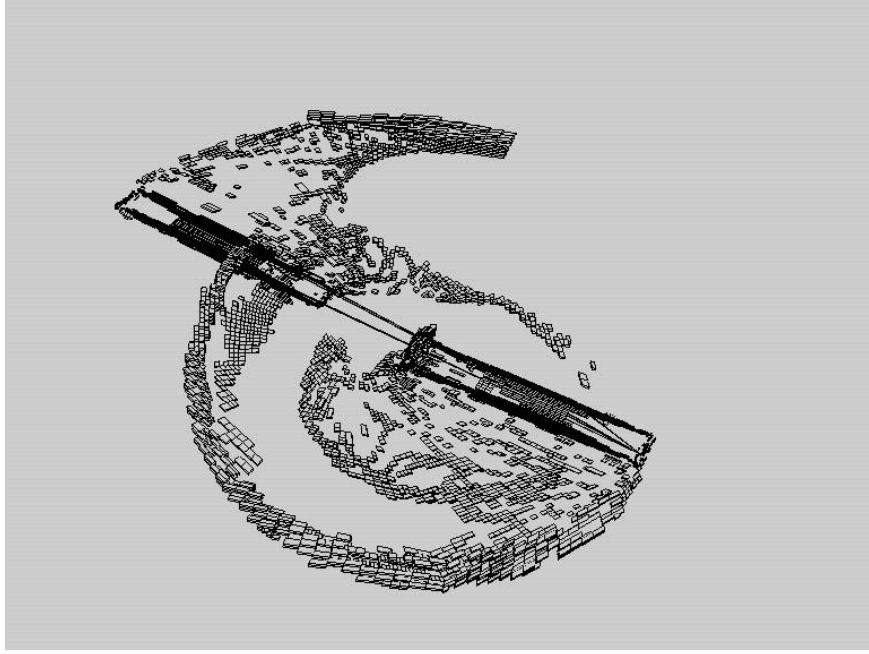


Figure 15. Four-dimensional simulation of the Operational Loads Survey rotor in forward flight. Full space grid of adapted grid in intermediate time level at azimuth $\psi = 151.25^\circ$. This intermediate time level has completely been generated by local grid refinement in time. ($M_{\text{tip}} = 0.664$, advance ratio 0.164, and thrust 0.0054). From van der Ven and Boelens (2003).

projection of $u_0|_{I_j}$ on the space $\mathbb{P}_k(I_j)$, that is, it is the only element of $\mathbb{P}_k(I_j)$ such that

$$(u_h(\cdot, 0), v)_{I_j} = (u_0, v)_{I_j} \quad (9)$$

for all $v \in \mathbb{P}_k(I_j)$. For $t > 0$, we take the approximate solution $u_h(\cdot, t)|_{I_j}$ to be the element of $\mathbb{P}_k(I_j)$ such that

$$(u_h(\cdot, t))_t, v)_{I_j} - (f(u_h(\cdot, t)), v_x)_{I_j} + \left\langle \widehat{f}(u_h(\cdot, t)) n_{I_j}, v \right\rangle_{\partial I_j} = 0, \quad (10)$$

for all $v \in \mathbb{P}_k(I_j)$, where $\widehat{f}(u_h)$ is the numerical flux which can be taken as indicated in the previous subsection. This completes the definition of the DG space discretization.

Note that, thanks to the fact that the approximations are discontinuous, the mass matrix is block diagonal, each block being of order $(k + 1)$. Moreover, this matrix can be rendered diagonal if we use (properly mapped) Legendre polynomials. Indeed, if, for $x \in I_j$, we write

$$u_h(x, t) = \sum_{\ell=0}^k u_j^\ell \varphi_\ell^j(x), \quad \varphi_\ell^j(x) = P_\ell(2(x - x_j)/\Delta_j), \quad \Delta_j = x_{j+1/2} - x_{j-1/2},$$

then, the initial condition (9) becomes

$$u_j^\ell(0) = \frac{(2\ell + 1)}{\Delta_j} \int_{I_j} u_0(x) \varphi_\ell^j(x) dx, \quad \ell = 0, \dots, k,$$

and the weak formulation (10) takes the following simple form:

$$\frac{d}{dt}u_j^\ell(t) + \frac{(2\ell+1)}{\Delta_j} \left(-(f(u_h(\cdot, t)) (\varphi_\ell^j)_x)_{I_j} + \langle \widehat{f}(u_h(\cdot, t)), \varphi_\ell^j \rangle_{\partial I_j} \right) = 0,$$

for $\ell = 0, \dots, k$.

Note that when $f(u) = u$, the system of equations for the degrees of freedom are:

$$\frac{d}{dt}u_j^\ell(t) + \frac{(2\ell+1)}{\Delta_j} \left(\sum_{m=0}^{\ell-1} (-1)^{\ell+m} u_j^m + \sum_{m=\ell}^k u_j^m - \sum_{m=0}^k (-1)^\ell u_{j-1}^m \right) = 0,$$

for $\ell = 0, \dots, k$.

Let us verify that the approximate solution remains bounded in the L^2 -norm. It is easy to see that the exact solution satisfies

$$\frac{d}{dt} \|u(\cdot, t)\|_{L^2(0,1)}^2 = 0.$$

The approximate solution satisfies, instead

$$\frac{d}{dt} \|u_h(\cdot, t)\|_{L^2(0,1)}^2 + \Theta_h(u_h(\cdot, t)) = 0,$$

where

$$\Theta_h(v) = \sum_{i=1}^N \left(\int_{u_h^-}^{u_h^+} (f(s) - \widehat{f}(u_h^-, u_h^+)) ds \right) (x_{i+1/2}) \geq 0.$$

For details, see Jiang and Shu (1994); see also Cockburn and Gremaud (1996).

3.5.2. The SSP-RK time discretization We discretize in time by using the following \mathcal{K} -stage SSP-RK method:

1. Set $u_h^{(0)} = u_h^n$;
2. For $i = 1, \dots, \mathcal{K}$ compute the intermediate functions:

$$u_h^{(i)} = \sum_{l=0}^{i-1} \alpha_{il} w_h^{il}, \quad w_h^{il} = u_h^{(l)} + \frac{\beta_{il}}{\alpha_{il}} \Delta t^n L_h(u_h^{(l)});$$

3. Set $u_h^{n+1} = u_h^{\mathcal{K}}$.

The method is called SSP if

- (i) If $\beta_{il} \neq 0$ then $\alpha_{il} \neq 0$,
- (ii) $\alpha_{il} \geq 0$,
- (iii) $\sum_{l=0}^{i-1} \alpha_{il} = 1$.

These methods were originally called TVD-RK methods as they preserved the TVD property of numerical schemes for non-linear conservation laws. They were introduced by Shu (1988) and by Shu and Osher (1988). Examples are displayed in Table II; more can be found in the paper by Gottlieb and Shu (1998). See also the recent review by Gottlieb et al. (2000).

Table II. TVD-RK time discretization parameters.

order	α_{il}	β_{il}	$\max\{\beta_{il}/\alpha_{il}\}$
2	$\begin{matrix} 1 \\ \frac{1}{2} \ \frac{1}{2} \end{matrix}$	$\begin{matrix} 1 \\ 0 \ \frac{1}{2} \end{matrix}$	1
3	$\begin{matrix} 1 \\ \frac{3}{4} \ \frac{1}{4} \\ \frac{1}{3} \ 0 \ \frac{2}{3} \end{matrix}$	$\begin{matrix} 1 \\ 0 \ \frac{1}{4} \\ 0 \ 0 \ \frac{2}{3} \end{matrix}$	1

The main property of these methods is that their stability *follows* from the stability of the forward Euler steps $w_h^{il} = u_h^{(l)} + \frac{\beta_{il}}{\alpha_{il}} \Delta t^n$. Indeed, assume that each of the Euler steps satisfy the following stability property

$$|w_h^{il}| \leq |u_h^{(l)}|,$$

for some semi-norm $|\cdot|$. Then

$$\begin{aligned} |u_h^{(i)}| &= \left| \sum_{l=0}^{i-1} \alpha_{il} w_h^{il} \right|, \\ &\leq \sum_{l=0}^{i-1} \alpha_{il} |w_h^{il}|, && \text{by the positivity property (ii),} \\ &\leq \sum_{l=0}^{i-1} \alpha_{il} |u_h^{(l)}|, && \text{by the stability assumption,} \\ &\leq \max_{0 \leq l \leq i-1} |u_h^{(l)}|, && \text{by the consistency property (iii).} \end{aligned}$$

It is clear now that that the inequality $|u_h^n| \leq |\mathbb{P}_h u_0|$, $\forall n \geq 0$, follows from the above inequality by a simple induction argument.

It is well known that the L^2 -stability of the method (in the linear case) is necessary in order to prevent the growth of the round-off errors. Such a stability property is usually achieved under a condition of the form

$$|c| \frac{\Delta t}{\Delta x} \leq \text{CFL}_{L^2}.$$

In Table III, we display the numbers CFL_{L^2} for a wide variety of time and space discretizations; they have been obtained by numerically. The symbol ‘ \star ’ indicates that the method is *unstable* when the ratio $\Delta t/\Delta x$ is held constant. For DG discretizations using polynomials of degree k and a $k+1$ stage RK method of order $k+1$ (which give rise to an $(k+1)$ -th order accurate method), we can take

$$\text{CFL}_{L^2} = \frac{1}{2k+1}.$$

Table III. The CFL_{L²} numbers for polynomials of degree k and RK methods of order ν .

k	0	1	2	3	4	5	6	7	8
$\nu = 1$	1.000	*	*	*	*	*	*	*	*
$\nu = 2$	1.000	0.333	*	*	*	*	*	*	*
$\nu = 3$	1.256	0.409	0.209	0.130	0.089	0.066	0.051	0.040	0.033
$\nu = 4$	1.392	0.464	0.235	0.145	0.100	0.073	0.056	0.045	0.037
$\nu = 5$	1.608	0.534	0.271	0.167	0.115	0.085	0.065	0.052	0.042
$\nu = 6$	1.776	0.592	0.300	0.185	0.127	0.093	0.072	0.057	0.047
$\nu = 7$	1.977	0.659	0.333	0.206	0.142	0.104	0.080	0.064	0.052
$\nu = 8$	2.156	0.718	0.364	0.225	0.154	0.114	0.087	0.070	0.057
$\nu = 9$	2.350	0.783	0.396	0.245	0.168	0.124	0.095	0.076	0.062
$\nu = 10$	2.534	0.844	0.428	0.264	0.182	0.134	0.103	0.082	0.067
$\nu = 11$	2.725	0.908	0.460	0.284	0.195	0.144	0.111	0.088	0.072
$\nu = 12$	2.911	0.970	0.491	0.303	0.209	0.153	0.118	0.094	0.077

The issue of the stability of the Euler forward step $w_h = u_h + \delta \Delta t^n L(u_h)$, where δ is a positive parameter, is by far more delicate. Indeed, from Table III, we see that this step is *always unstable* in L^2 . On the other hand, when the method uses piecewise-constant approximations, then the forward Euler step is nothing but a monotone scheme which are total variation diminishing (TVD), that is,

$$|w_h|_{TV(0,1)} \leq |u_h|_{TV(0,1)},$$

where

$$|u_h|_{TV(0,1)} \equiv \sum_{1 \leq j \leq N} |u_{j+1} - u_j|,$$

is the total variation of u_h . Hence, if we use piecewise polynomial approximations, it is reasonable to try to see if the Euler forward step under consideration is stable for the following seminorm

$$|u_h|_{TVM(0,1)} \equiv \sum_{1 \leq j \leq N} |\bar{u}_{j+1} - \bar{u}_j|,$$

where \bar{u}_j is the mean of u_h in the interval I_j . Thus, this semi-norm is the total variation of the local means of u_h . The following result give the conditions for the Euler forward step to be non-expansive with respect to this semi-norm.

Proposition 3.1 (The sign conditions) *We have*

$$|w_h|_{TVM(0,1)} \leq |u_h|_{TVM(0,1)},$$

provided that

$$\begin{aligned} \text{sign}(u_{j+1/2}^+ - u_{j-1/2}^+) &= \text{sign}(u_{j+1}^0 - u_j^0), \\ \text{sign}(u_{j+1/2}^- - u_{j-1/2}^-) &= \text{sign}(u_j^0 - u_{j-1}^0), \end{aligned}$$

and provided that

$$|\delta| \left(\frac{|\hat{f}(a, \cdot)|_{Lip}}{\Delta_{j+1}} + \frac{|\hat{f}(\cdot, b)|_{Lip}}{\Delta_j} \right) \leq 1.$$

This result states that a discretization in space by the DG method and an SSP-RK time discretization of the resulting system of ordinary differential equations does not guarantee a non-expansive total variation in the local means. Fortunately, the sign conditions can be enforced by a generalized slope limiter, $\Lambda\Pi_h$.

3.5.3. The generalized slope limiter Next, we construct the operator $\Lambda\Pi_h$; set $u_h = \Lambda\Pi_h v_h$. To do that, let us denote by v_h^1 the L^2 -projection of v_h into the space of piecewise-linear functions. We then define $u_h = \Lambda\Pi_h(v_h)$ on the interval I_j , as follows:

(i) Compute

$$\begin{aligned} u_{j+1/2}^- &= \bar{v}_j + m(v_{j+1/2}^- - \bar{v}_j, \bar{v}_j - \bar{v}_{j-1}, \bar{v}_{j+1} - \bar{v}_j) \\ u_{j-1/2}^+ &= \bar{v}_j - m(\bar{v}_j - v_{j-1/2}^+, \bar{v}_j - \bar{v}_{j-1}, \bar{v}_{j+1} - \bar{v}_j). \end{aligned}$$

- (ii) If $u_{j+1/2}^- = v_{j+1/2}^-$ and $u_{j-1/2}^+ = v_{j-1/2}^+$, set $u_h|_{I_j} = v_h|_{I_j}$,
 (iii) If not, take $u_h|_{I_j}$ equal to $\Lambda\Pi_h^O(v_h^1)$.

This generalized slope limiter does not degrade the accuracy of the scheme, except at critical points. In order to avoid that, we replace the *minmod* function m by the *corrected minmod* function \bar{m}_j defined by

$$\bar{m}_j(a_1, a_2, a_3) = \begin{cases} a_1 & \text{if } |a_1| \leq M\Delta_j^2, \\ m(a_1, a_2, a_3) & \text{otherwise,} \end{cases}$$

where M is an upper bound of the absolute value of the second-order derivative of the solution at local extrema.

We have the following result.

Proposition 3.2 (The TVBM property) Suppose that for $j = 1, \dots, N$

$$|\delta| \left(\frac{|\hat{f}(a, \cdot)|_{Lip}}{\Delta_{j+1}} + \frac{|\hat{f}(\cdot, b)|_{Lip}}{\Delta_j} \right) \leq 1/2.$$

Then, if $u_h = \Lambda\Pi_{h,M} v_h$, then

$$|\bar{w}_h|_{TVM(0,1)} \leq |\bar{u}_h|_{TVM(0,1)} + C M \Delta x.$$

Note that the condition on δ is independent of the form that the approximate solution has in space.

3.5.4. The non-linear stability of the RKDG method For this method, we have the following stability result.

Theorem 3.3 (TVBM-stability of the RKDG method) *Let each time step Δt^n satisfy the following CFL condition:*

$$\max_{il} \left| \frac{\beta_{il}}{\alpha_{il}} \right| \Delta t^n \left(\frac{|\widehat{f}(a, \cdot)|_{Lip}}{\Delta_{j+1}} + \frac{|\widehat{f}(\cdot, b)|_{Lip}}{\Delta_j} \right) \leq 1/2. \quad (11)$$

Then we have

$$|\bar{u}_h^n|_{TVM(0,1)} \leq |u_0|_{TV(0,1)} + CMQ \quad \forall n = 0, \dots, L,$$

where $L \Delta x \leq Q$.

Let us emphasize that, as we have seen, the DG space discretization, the RK time discretization and the generalized slope limiter are inter-twined just in the right way to achieve the above non-linear stability result. Thus, although the DG space discretization of this method is an essential distinctive feature, the other two ingredients are of no less relevance.

Note that the above result holds for any polynomial degree and for any order of accuracy in time. This shows that this stability result does not impose an accuracy barrier to the method, as happens with many other methods. The RKDG method can actually achieve high-order accuracy when the exact solution is smooth because the generalized slope limiter does not degrade the high-order accuracy of the space and time discretizations. Although there are no theoretical error estimates that justify this above statement, it is actually supported by overwhelming practical evidence.

Note also that for the linear case $f(u) = cu$, the CFL condition (11) becomes

$$|c| \frac{\Delta t}{\Delta x} \leq \text{CFL}_{\text{TV}} \equiv \frac{1}{2 \max_{il} \frac{\beta_{il}}{\alpha_{il}}}.$$

In general, the restriction of the time step imposed by the TVBM property is *much weaker* than that required to achieve L^2 -stability. However, it is the condition for L^2 stability that needs to be respected; otherwise, the round-off errors would get amplified and the high-order accuracy of the method would degenerate even though the RKDG method remains TVBM-stable.

It is not difficult to use Theorem 3.3 to conclude, by using a discrete version of the Ascoli-Arzelá theorem, that from the sequence $\{\bar{u}_h\}_{\Delta x > 0}$, it is possible to extract a subsequence strongly converging in $L^\infty(0, T; L^1(0, 1))$ to a limit u^* . That this limit is a weak solution of the non-linear conservation law can be easily shown. However, while there is ample numerical evidence that suggests that u^* is actually the entropy solution, this fact remains a very challenging theoretical open problem.

3.6. RKDG methods for multi-dimensional hyperbolic systems

The extension of the RKDG methods to the model multi-dimensional hyperbolic system

$$\mathbf{u}_t + \sum_{i=1}^N (\mathbf{f}_i(\mathbf{u}))_{x_i} = \mathbf{0},$$

deserves comments on a few key points.

3.6.1. The basis functions Just like in the one dimensional case, the mass matrix is block-diagonal; the block associated with the element K is a square matrix of order equal to the dimension of the local space and hence can be easily inverted. Moreover, for a variety of elements and spaces, a basis can be found which is orthonormal in L^2 . This is the case, for example, of rectangles and tensor product polynomials, in which case the orthonormal basis is a properly scaled tensor product of Legendre polynomials. For simplices and polynomials of a given total degree, there is also an orthonormal basis; see the work by Dubiner (1991), by Karniadakis and Sherwin (1999) and Warburton (1998), and the recent implementations by Aizinger et al. (2000) and Hesthaven and Warburton (2002).

3.6.2. Quadrature rules In practice, the integrals appearing in the weak formulation need to be approximated by quadrature rules. It was proven by Cockburn et al. (1990) that

$$\|L_h(u) + \nabla \cdot f(u)\|_{L^\infty(K)} \leq C h^{k+1} |f(u)|_{W^{k+2,\infty}(K)},$$

if the quadrature rules over each of the faces of the border of the element K are exact for polynomials of degree $2k+1$, and if the one over the element is exact for polynomials of degree $2k$. The fact that these requirements are also necessary, can be easily numerically verified; moreover, the method is more sensitive to the quality of the quadrature rules used on the boundary of the elements than to that used in their interior.

Finally, let us point out that a quadrature-free version of the method was devised by Atkins and Shu (1998) which results in a very efficient method for linear problems and certain nonlinear problems such as Euler equations of gas dynamics. A very efficient quadrature rule was obtained by van der Ven and van der Vegt (2002) for the Euler equations of gas dynamics by suitably exploiting the structure of the equations.

3.6.3. Numerical fluxes When dealing with multi-dimensional hyperbolic systems, the so-called local Lax-Friedrichs numerical flux is a particularly convenient choice of numerical flux. Indeed, it can be easily applied to any non-linear hyperbolic system, it is simple to compute, and yields good results. This numerical flux is defined as follows. If we set $\mathbf{f}_{\mathbf{n}_K} = \sum_{i=1}^N n_i \mathbf{f}_i(\mathbf{u})$, we define the local Lax-Friedrichs numerical flux as

$$\widehat{\mathbf{f}}_{\mathbf{n}_K}^{LLF}(\mathbf{u}_h) = \{\mathbf{f}_{\mathbf{n}_K}(\mathbf{u}_h)\} - \frac{C}{2} \llbracket \mathbf{u}_h \rrbracket_{\mathbf{n}_K},$$

where $C = C(K^\pm)$ is the larger one of the largest eigenvalue (in absolute value) of $\frac{\partial}{\partial \mathbf{u}^\pm} \mathbf{f}_{\mathbf{n}_{K^\pm}}(\mathbf{u}^\pm)$, or, in practice, of $\frac{\partial}{\partial \mathbf{u}^\pm} \mathbf{f}_{\mathbf{n}_{K^\pm}}(\bar{\mathbf{u}}_{K^\pm})$, where $\bar{\mathbf{u}}_{K^\pm}$ are the means of the approximate solution \mathbf{u}_h in the elements K^\pm .

For symmetric hyperbolic systems, it is possible to devise numerical fluxes that render the method of lines (or the space-time methods) L^2 -stable; see Barth (2000).

3.6.4. The slope limiter $\Lambda \Pi_h$ When we dealt with the scalar one dimensional conservation law, the role of the generalized slope limiter $\Lambda \Pi_h$ was to enforce the TVBM property of a typical Euler forward time step. In the case of multi-dimensional scalar conservation laws, we cannot rely anymore on the TVBM property of the Euler forward step because such a property does not hold for monotone schemes on general meshes; it has been proven only for monotone schemes in non-uniform Cartesian grids by Sanders (1983). We can, instead, rely on a local maximum principle; see the paper by Cockburn et al. (1990).

A practical and effective generalized slope limiter $\Lambda\Pi_{h,M}$ was later developed by Cockburn and Shu (1998b). To apply it to the function v_h , we proceed on the element K as follows:

- (i) Compute the L^2 -projection of v_h into the linear functions on K , $v_h^1|_K$,
- (ii) Compute $r_h|_K = \Lambda\Pi_{h,M}^1 v_h^1|_K$,
- (iii) If $r_h|_K = v_h^1|_K$, set $u_h|_K = v_h|_K$,
- (iv) If not, set $u_h|_K = r_h|_K$.

Note that in order to use this generalized slope limiter, one only needs to know how to slope limit piecewise linear functions; for the details of the definition of $\Lambda\Pi_{h,M}^1$, we refer the reader to the paper by Cockburn and Shu (1998b).

An interesting limiter has been proposed by Wierse (1997). Kershaw et al. (1998) introduced a limiter based on quadratic programming. Biswas et al. (1994) devised a limiter based on local moments, rather than on slopes, and used it for adaptivity purposes. More recently, Burbeau et al. (2001) proposed what they call a *problem-independent* slope limiter.

3.6.5. Characteristic variables For systems, limiting in the local characteristic variables gives remarkably superior results than doing it component-by-component.

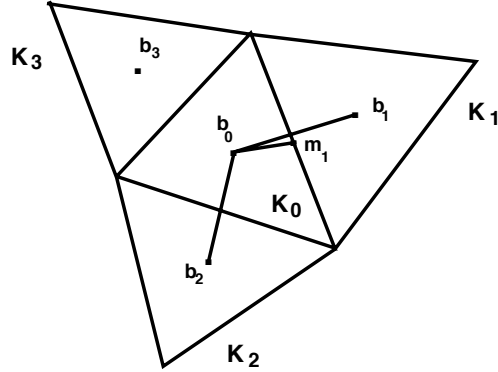


Figure 16. Illustration of limiting.

To limit the vector $\tilde{v}_h(m_i, K_0)$ in the element K_0 , see Fig. 16, we proceed as follows:

- Find the matrix R and its inverse R^{-1} , which diagonalizes the Jacobian

$$J = \frac{\partial}{\partial u} f(\bar{v}_{K_0}) \cdot \frac{m_i - b_0}{|m_i - b_0|},$$

that is, $R^{-1} J R = \Lambda$, where Λ is a diagonal matrix containing the eigenvalues of J . Notice that the columns of R are the right eigenvectors of J and the rows of R^{-1} are the left eigenvectors.

- Transform $\tilde{v}_h(m_i, K_0)$ and $\Delta\bar{v}(m_i, K_0)$ to the characteristic fields. This is achieved by left multiplying these vectors by R^{-1} .

- Apply the scalar limiter to each of the components of the transformed vectors.
- Multiply by R on the left to transform the result back to the original space.

3.7. Computational results

In this subsection, we display computational results that show that the RKDG method can achieve exponential convergence when the solution is very smooth and that it can perform as well as the high-resolution methods when discontinuities are present. We also show results showing its excellent handling of boundary conditions and its remarkable parallelization properties. Finally, we also show that the use of higher degree polynomials results in a more efficient method, even in the presence of discontinuities.

3.7.1. Exponential convergence To show that exponential convergence can be achieved and that it is always more efficient to use higher degree polynomials when the exact solution is very smooth, we consider

$$u_t + \nabla \cdot (\mathbf{v} u) = 0$$

where $\mathbf{v} = 2\pi(-y, x)$ and the initial condition is a Gaussian hill. In Fig. 17, we see the L^2 -error at time $T = 1$ versus the CPU time for the four different successively refined meshes described below and for polynomials of degree up to six. The refinement of the mesh is obtained by dividing the triangles in four congruent triangles. Each line corresponds to a different mesh, with the symbols on each line representing the error for the six different approximating spaces. We easily observe that exponential convergence is achieved and that it is always more efficient to use a coarser mesh with a higher order polynomial approximation.

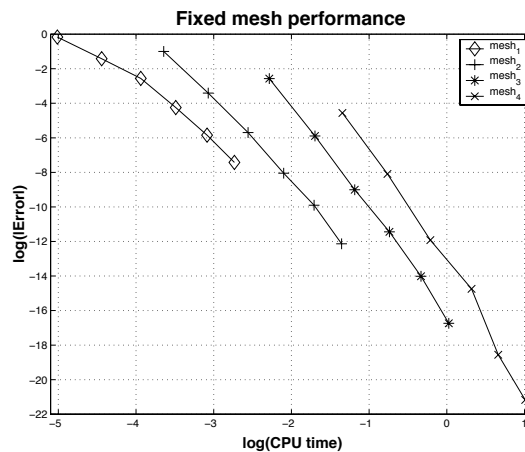


Figure 17. Spectral convergence and comparison of L^2 -error versus CPU time for 4 successively refined meshes and polynomials of degree 1 to 6. From Aizinger et al. (2000)

3.8. Treatment of the boundary conditions

To show the ease with which the method deals with the boundary conditions, we consider a variation of the above problem

$$u_t + \nabla \cdot (\mathbf{v} u) = 0.$$

where $\mathbf{v} = (-y + 1/2, x - 3/4)$ and the initial data is

$$u(\mathbf{x}, t = 0) = \begin{cases} \exp\left(8 - \frac{8}{1-8|\mathbf{x}-(3/4,1)|^2}\right), & \text{if } 8|\mathbf{x} - (3/4, 1)|^2 < 1, \\ 0, & \text{otherwise.} \end{cases}$$

An RKDG method using quadratic polynomial approximations and a SSP-RK method of order three is used. Note that, unlike the previous example, only part of the initial data is in the computational domain. The boundary conditions are taken by using the Lax-Friedrichs flux and by giving the exact solution as the exterior trace. In Table 3.8, we see that the full order three has been achieved, as expected. In Fig. 18, we also see that the boundary conditions have been captured very well by the RKDG method.

Table IV. Errors at $T = \frac{3}{4}\pi$

mesh	$\ e_u(T)\ _{L^\infty(\Omega)}$	order	$\ e_u(T)\ _{L^1(\Omega)}$	order
16×16	0.21E-01	2.01	0.42E-03	3.32
32×32	0.25E-02	3.07	0.42E-04	3.31
64×64	0.32E-03	2.96	0.49E-05	3.11
128×128	0.52E-04	2.64	0.60E-06	3.01

3.8.1. Approximation of contact discontinuities Let us now show how the contact discontinuities are approximates by the RKDG methods. To do that, we consider the problem

$$u_t + u_x = 0, \quad \text{in } [0, 1) \times (0, T),$$

with periodic boundary conditions and initial condition

$$u(x, 0) = \begin{cases} 1, & \text{if } x \in (.25, .75), \\ 0, & \text{otherwise.} \end{cases}$$

In Figs. 19 and 20, we show the results given by RKDG methods using polynomials of degree k and a $(k + 1)$ -stage, $(k + 1)$ th-order accurate SSP-RK method. We see that as the polynomials degree increases, so does the quality of the approximation of the contact discontinuity, except, perhaps for the unwanted oscillations near them.

3.8.2. Approximation of shocks First, let us show in a simple example that the RKDG methods can capture shocks as well as any high-resolution finite difference or finite volume scheme. Consider the approximation of the entropy solution of the inviscid Burgers equation

$$u_t + (u^2/2)_x = 0,$$

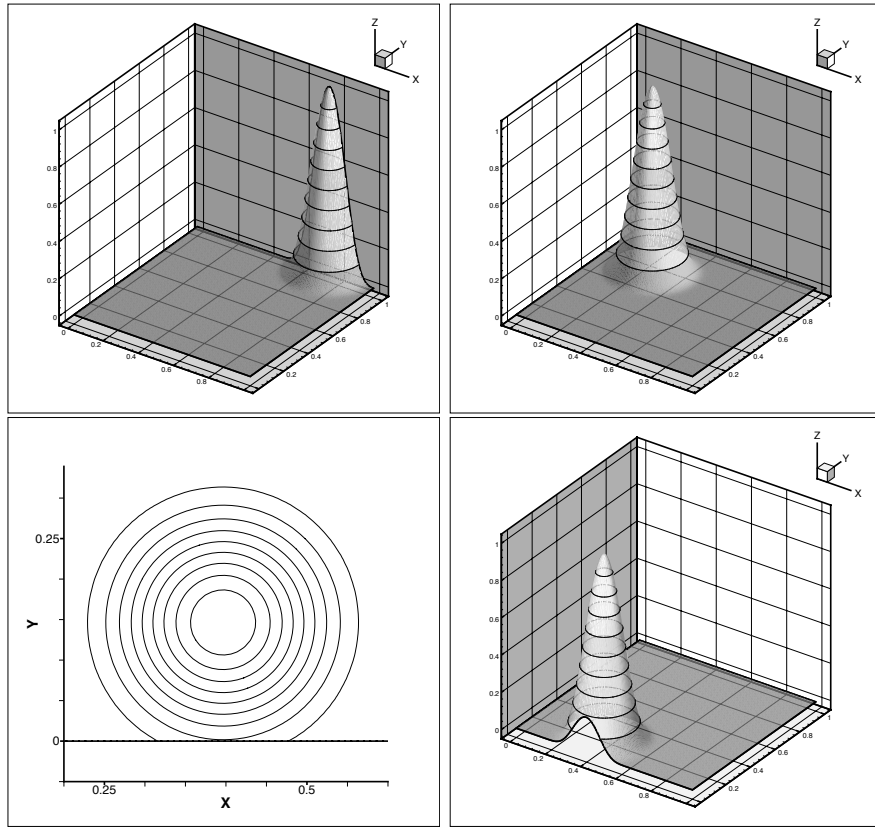


Figure 18. Approximate solution at $T = 0.0$ (top left), $T = \frac{3}{8}\pi$ (top right) and $T = \frac{3}{4}\pi$ (bottom). The mesh is a uniform 64×64 of triangles.

on the domain $(0, 1) \times (0, T)$ with initial condition $1/4 + \sin(\pi(2x-1))/2$ and periodic boundary conditions. In Fig. 21, we display the RKDG solution using piecewise linear and piecewise quadratic approximations; note how, in both cases, the shock has been captured within three elements as would be expected of any high-resolution scheme.

3.8.3. Parallelizability Let us address the parallelizability of the RKDG method. In Table V below, we display the results obtained by Biswas et al. (1994); we see the solution time and total execution time for the two-dimensional problem

$$u_t + u_x + u_y = 0,$$

on the domain $(-\pi, \pi)^2 \times (0, T)$ with initial condition $u(x, y, 0) = \sin(\pi x) \sin(\pi y)$ and periodic boundary conditions. Biswas et al. (1994) used 256 elements per processor and ran the RKDG method with polynomials of degree two and 8 time steps; the work per processor was kept constant. Note how the solution time increases only slightly with the number of processors and the remarkable parallel efficiency of the method.

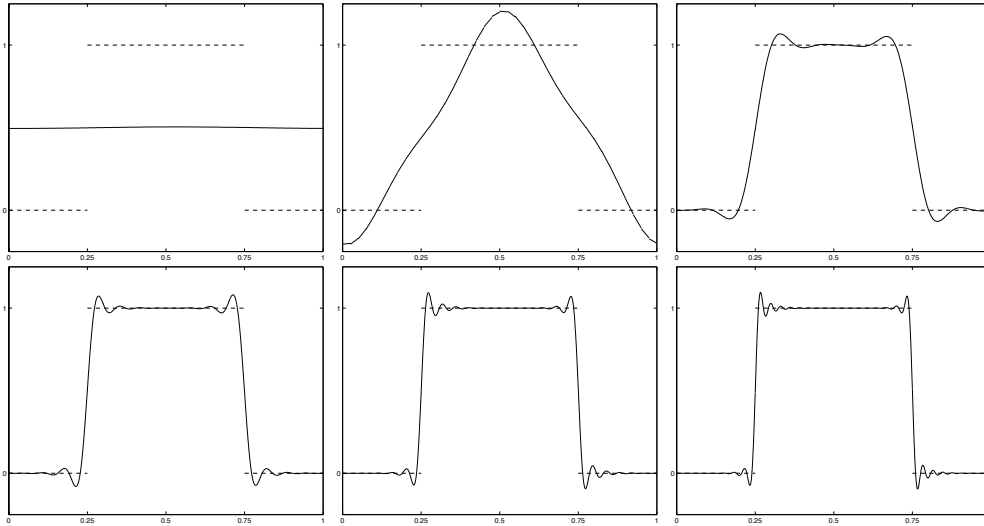


Figure 19. Effect of the order of the RKDG method on the approximation of discontinuities. The exact solution at time $T = 100$, u (dashed line), is contrasted against the approximate solution u_h (solid line) obtained with the RKDG method of order $k + 1$ on a mesh of 40 elements for the values $k = 0$ (left top), $k = 1$ (middle top), $k = 2$ (right top), $k = 3$ (left middle), $k = 4$ (middle middle), and $k = 5$ (right middle). No limiter was used. From Cockburn and Shu (2001).

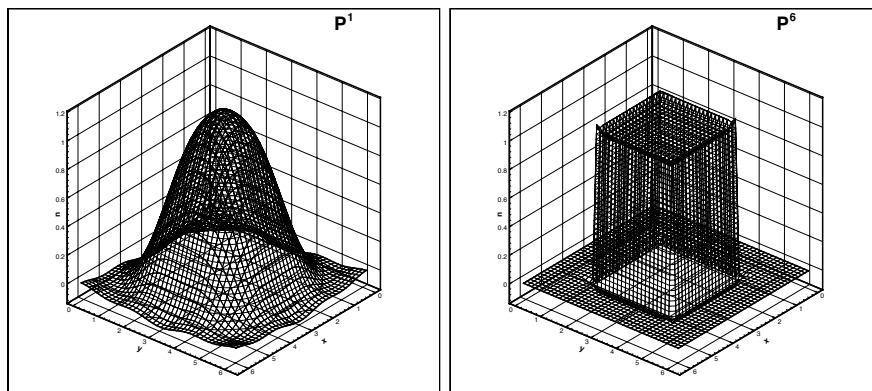


Figure 20. Effect of the order of the RKDG method on the approximation of discontinuities. Comparison of the exact and the RKDG solutions at $T = 100\pi$ with $k = 1$ (left bottom) and $k = 6$ (right bottom). Two dimensional results with 40×40 squares. No limiter was used. From Cockburn and Shu (2001).

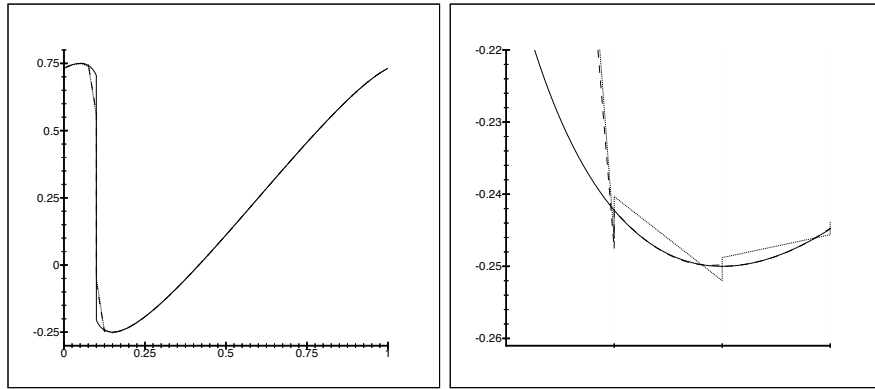


Figure 21. Burgers equation: Comparison of the exact and the RKDG solutions obtained with $\Delta x = 1/40$ at $T = 0.40$. Full domain (left) and zoom on three elements (right) the first of which contains the exact shock. Exact solution (solid line), piecewise linear approximation (dotted line), and piecewise quadratic approximation (dashed line). From Cockburn (1999).

Table V. Scaled parallel efficiency. Solution times (without I/O) and total execution times measured on the nCUBE/2. From Biswas et al. (1994).

Number of processors	Work (W)	Solution time (secs.)	Solution parallel efficiency	Total time (secs.)	Total parallel efficiency
1	18,432	926.92	-	927.16	-
2	36,864	927.06	99.98%	927.31	99.98%
4	73,728	927.13	99.97%	927.45	99.96%
8	147,456	927.17	99.97%	927.58	99.95%
16	294,912	927.38	99.95%	928.13	99.89%
32	589,824	927.89	99.89%	929.90	99.70%
64	1,179,648	928.63	99.81%	931.28	99.55%
128	2,359,296	930.14	99.65%	937.67	98.88%
256	4,718,592	933.97	99.24%	950.25	97.57%

3.8.4. Approximation of complex solutions Let us show that the RKDG method can handle solutions with very complicated structure. Consider the classical double-Mach reflection problem for the Euler equations of gas dynamics. In Fig. 22, details of the approximation of the density are shown. Note that the strong shocks are very well resolved by the RKDG solution using piecewise linear and piecewise quadratic polynomials defined on *squares*. Also, note that there is a remarkable improvement in the approximation of the density near the contacts when going from linear to quadratic polynomials.

A similar conclusion can be drawn in the case of the flow of a gas past a forward facing step; see, for example, the study by Woodward and Colella (1984).

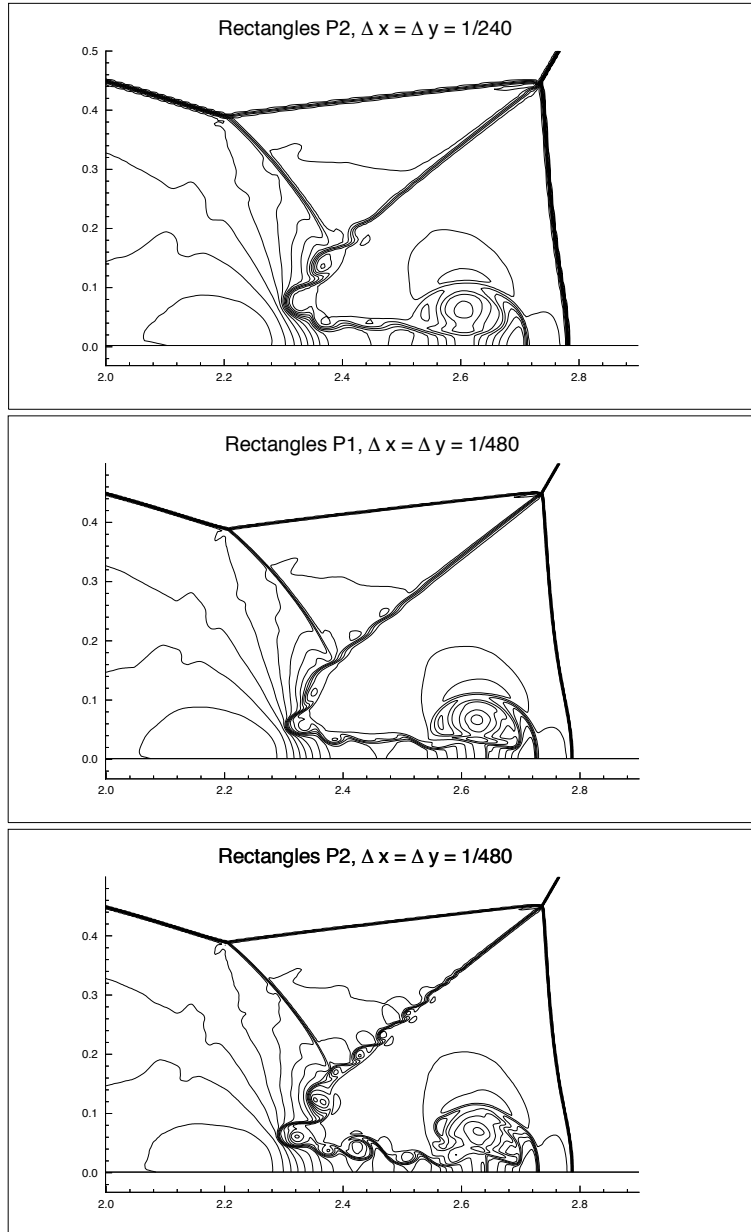


Figure 22. Euler equations of gas dynamics: Double Mach reflection problem. Isolines of the density around the double Mach stems. Quadratic polynomials on squares $\Delta x = \Delta y = \frac{1}{240}$ (top); linear polynomials on squares $\Delta x = \Delta y = \frac{1}{480}$ (middle); and quadratic polynomials on squares $\Delta x = \Delta y = \frac{1}{480}$ (bottom). From Cockburn and Shu (1998b).

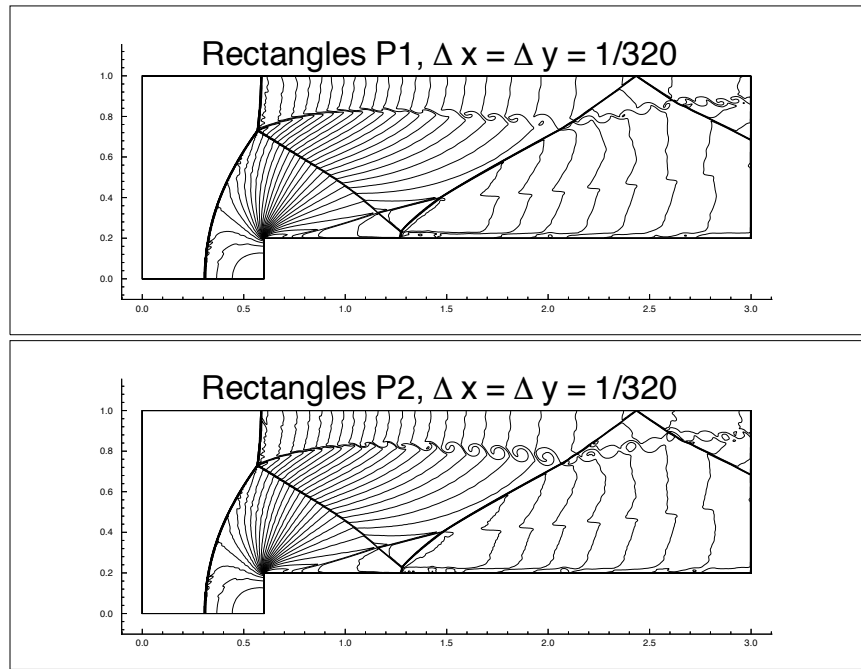


Figure 23. Forward facing step problem. Approximation of the density ρ . 30 equally spaced contour lines from $\rho = 0.090338$ to $\rho = 6.2365$. From Cockburn and Shu (1998b).

3.8.5. Problems with curved boundaries Bassi and Rebay (1997b) showed the importance of approximating as accurately as possible the boundaries of the physical domain and the ease with which this is achieved by using the RKDG methods. Indeed, for the classical two-dimensional isentropic flow around a circle, they showed that approximating the circle by a polygon results in non-physical entropy production at each of the kinks which is then carried downstream and accumulates into a non-physical wake which does not disappear by further refining the grid. However, by simply taking into account the exact shape of the boundary, a remarkably improved approximation is obtained; see Fig. 24.

On the other hand, van der Vegt and van der Ven (2002a) have recently shown that the high-order accurate representation of the curved boundary can be avoided by using local grid refinement.

3.8.6. Adaptivity for the Euler equations of gas dynamics Next, we give examples of adaptivity using the RKDG method with anisotropic mesh refinement. The first two examples illustrate the use of conforming mesh refinement. For the first example, two Sedov-type explosions in an open square domain develop and interact while bouncing on square obstacles and interacting with each other; see Fig. 25. In the second example, the blast of a cannon is simulated in order to understand the shape of the blast waves around the muzzle break; see Fig. 26.

Finally, we present an example of a steady-state computation on an ONERA M6 wing for

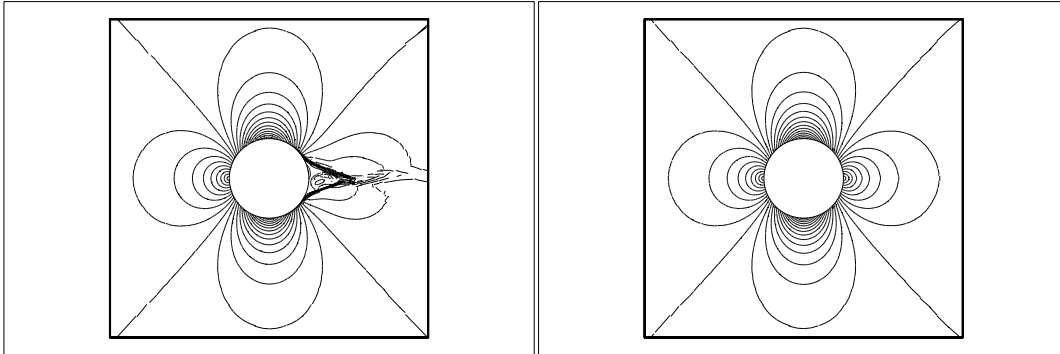


Figure 24. Mach isolines of the DG approximation with P^1 elements: The circle is approximated by a polygonal (top) and rendered exactly (bottom). From Bassi and Rebay (1997b).

which non-conforming refinement has been employed; see Fig. 27.

3.8.7. Simulation of inertial confinement fusion Our final example is the simulation of the implosion of a NIF capsule which consists of a nearly vacuum inner region enclosed by two spherical shells. For details, see Shestakov et al. (2001). This is a complicated and very difficult problem which involves the simulation of hydrodynamics, heat conduction and radiation transport phenomena. Only the hydrodynamics part of the problem is simulated by using a *one-step* ALE, RKDG method proposed by Kershaw et al. (1998) and implemented in the ICF3D code by Shestakov et al. (2000). In Fig. 28, we see the mesh and several physical quantities after 8 nano-seconds of having deposited energy on the outer surface of the capsule. Note the near spherical symmetry of the implosion.

4. DG methods for second-order elliptic problems

In this section, we consider DG methods for elliptic problems. We do this not only because this also has applications to fluid flow (in porous media, for example) but mainly as a much needed transition towards dealing with DG methods for convection-dominated flows. The emphasis here is on the fact that the numerical fluxes used in the framework of hyperbolic conservation laws do not need to be associated to approximate Riemann solvers. Instead, they are better understood if they are considered to be *numerical traces* that must be chosen in order to render the DG method both stable and accurate. We discuss how the various choices of numerical traces give rise to the main DG methods for these problems and discuss their corresponding properties. Finally, we show that, also in this context, the stability of the DG methods is enhanced by the jumps of the approximate solution and that this property establishes a link between them and the so-called stabilized mixed methods.

We present these ideas for the second-order elliptic model problem:

$$-\Delta u = f \quad \text{in } \Omega, \quad u = 0 \quad \text{on } \partial\Omega_{\mathcal{D}}, \quad \frac{\partial u}{\partial n} = \mathbf{g}_{\mathcal{N}} \cdot \mathbf{n} \quad \text{on } \partial\Omega_{\mathcal{N}},$$

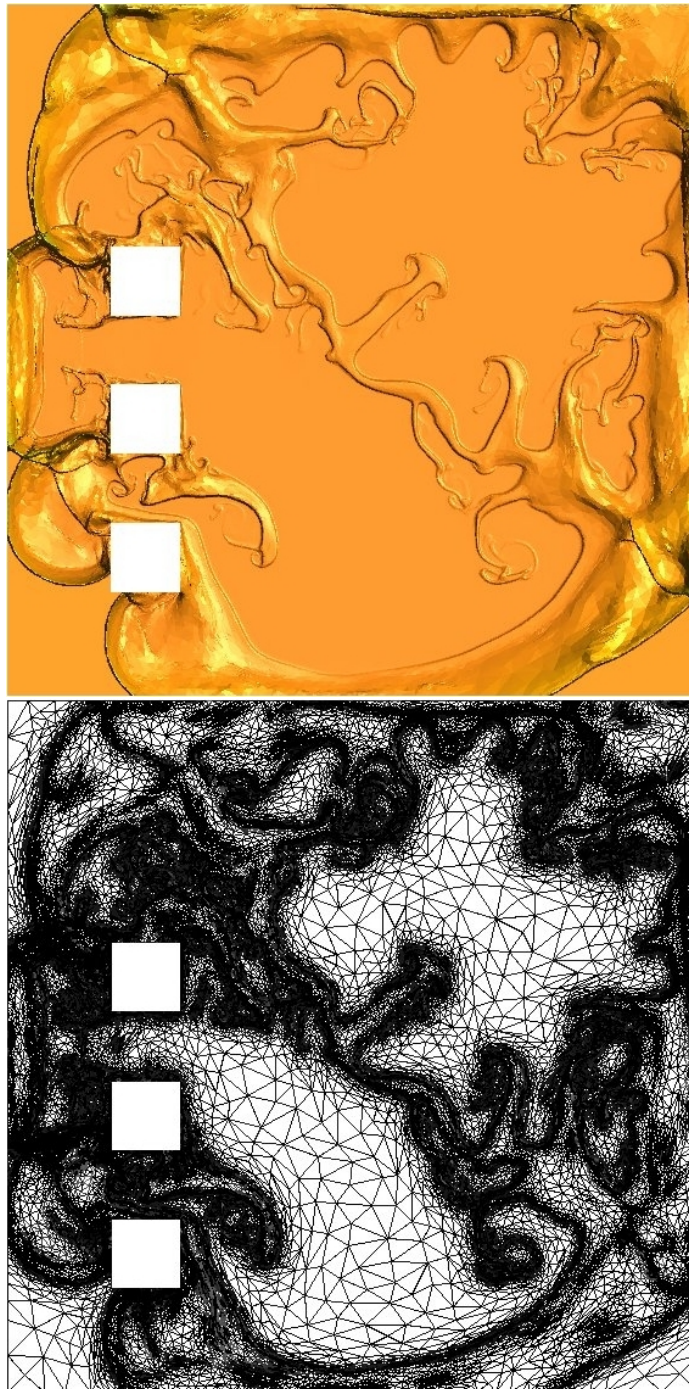


Figure 25. Two explosions in a square domain with obstacle: density (top), and the corresponding mesh (bottom) after 1 second. From Remacle et al. (2003).

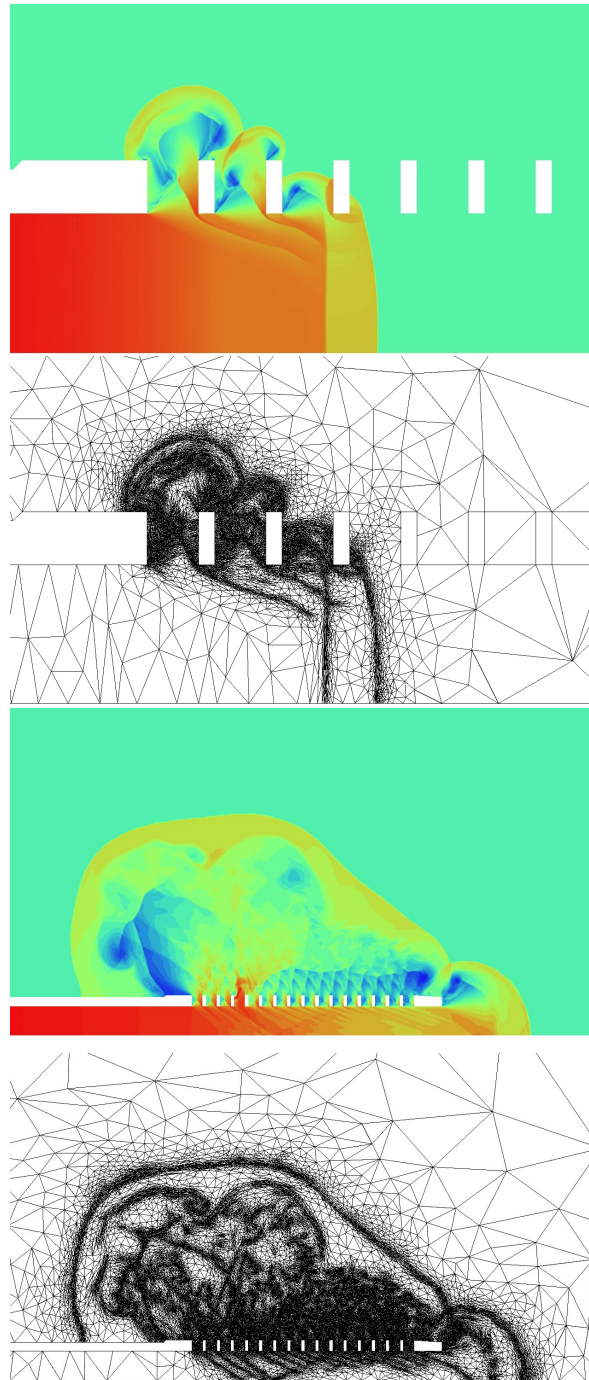


Figure 26. Cannon-Blast simulation: Density and the corresponding mesh. Close up on the muzzle break at an early stage (top), and after the main blast wave left the muzzle (bottom). From Remacle et al. (2003) *Encyclopedia of Computational Mechanics*. Edited by Erwin Stein, René de Borst and Thomas J.R. Hughes. © 2004 John Wiley & Sons, Ltd.

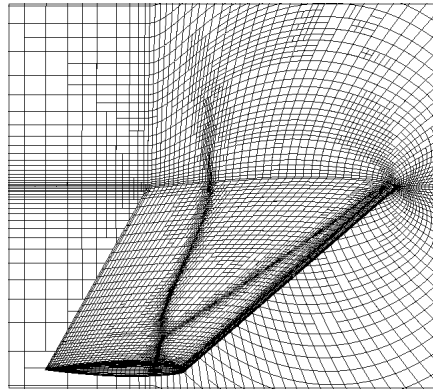


Figure 27. Final adapted grid on ONERA M6 wing, clearly showing the lambda shock (flow conditions $M_\infty = 0.84$, $\alpha = 3.06^\circ$). From van der Vegt and van der Ven (1998).

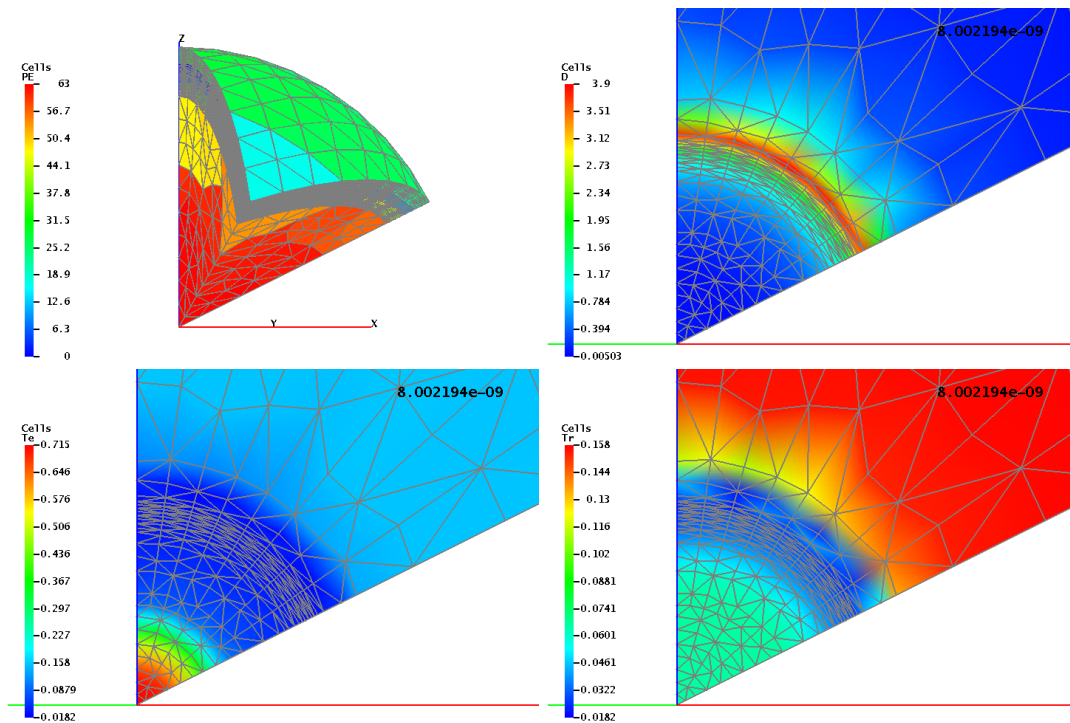


Figure 28. ICF capsule implosion: Mesh (top, left) with colours indicating to which processor the element belongs. Density (top, right), matter temperature (bottom, left), and radiation temperature (bottom, right) at 8 nano-seconds. From Shestakov et al. (2001).

where Ω is a bounded domain of \mathbb{R}^N , $\partial\Omega = \partial\Omega_{\mathcal{D}} \cup \partial\Omega_{\mathcal{N}}$, and \mathbf{n} is the outward unit normal to its boundary.

4.1. DG methods for the model problem

A way to define a DG method consists in rewriting the elliptic model problem as a system of first-order equations, namely,

$$\mathbf{q} = \nabla u, \quad -\nabla \cdot \mathbf{q} = f \quad \text{in } \Omega, \quad u = 0 \quad \text{on } \partial\Omega_{\mathcal{D}}, \quad \mathbf{q} \cdot \mathbf{n} = \mathbf{g}_{\mathcal{N}} \cdot \mathbf{n} \quad \text{on } \partial\Omega_{\mathcal{N}},$$

and then applying to it a DG discretization. Thus, the approximate solution (\mathbf{q}_h, u_h) on the element K is taken in the space $\mathcal{Q}(K) \times \mathcal{U}(K)$ and is determined by imposing that for all $(\mathbf{r}, v) \in \mathcal{Q}(K) \times \mathcal{U}(K)$,

$$\begin{aligned} \int_K \mathbf{q}_h \cdot \mathbf{r} \, dx &= - \int_K u_h \nabla \cdot \mathbf{r} \, dx + \int_{\partial K} \widehat{u_h \mathbf{n}_K} \cdot \mathbf{r} \, ds, \\ \int_K \mathbf{q}_h \cdot \nabla v \, dx &= \int_K f v \, dx + \int_{\partial K} v \widehat{\mathbf{q}_h \cdot \mathbf{n}_K} \, ds, \end{aligned}$$

where $\widehat{u_h \mathbf{n}_K}$ and $\widehat{\mathbf{q}_h \cdot \mathbf{n}_K}$ are the numerical fluxes.

Just as for DG methods for hyperbolic problems, the definition of the numerical fluxes determines the properties of the corresponding DG method. In this context, we also require that the numerical fluxes (i) depend only the traces of the approximation on the boundary of the elements, (ii) be consistent and, (iii) be conservative. As discussed previously, the first property renders the numerical traces easy to evaluate and ensures a high degree of locality of the method. The second, ensures the convergence of the method to the correct solution. The third property, which is highly valued in computational fluid dynamics, is also very important in this context. If violated, the method produces a stiffness matrix for the primal variable which is not symmetric; see the paper by Arnold et al. (2001) for a complete discussion. More importantly, it exhibits a loss in the rate of convergence in u_h as well as a significant degradation in the quality of the approximation of linear functionals as was recently shown by Harriman et al. (2003).

In order to fix ideas, let us consider the numerical fluxes of the local discontinuous Galerkin (LDG) introduced by Cockburn and Shu (1998a). First, we note that in this context, it is possible to rewrite the numerical fluxes as

$$\widehat{u_h \mathbf{n}_K} = \widehat{u}_{h,K} \mathbf{n}_K, \quad \widehat{\mathbf{q}_h \cdot \mathbf{n}_K} = \widehat{\mathbf{q}}_{h,K} \cdot \mathbf{n}_K,$$

where $\widehat{u}_{h,K}$ and $\widehat{\mathbf{q}}_{h,K}$ are the numerical traces. If we now introduce the notation

$$\llbracket u_h \rrbracket = u_h^+ \mathbf{n}^+ + u_h^- \mathbf{n}^-, \quad \text{and} \quad \llbracket \mathbf{q}_h \rrbracket = \mathbf{q}_h^+ \cdot \mathbf{n}^+ + \mathbf{q}_h^- \cdot \mathbf{n}^-, \quad \text{where} \quad \omega_h^\pm(\mathbf{x}) = \lim_{\epsilon \downarrow 0} \omega_h(\mathbf{x} - \epsilon \mathbf{n}^\pm),$$

the numerical traces of the LDG method are defined as follows. Inside the domain Ω , we take

$$\begin{aligned} \widehat{\mathbf{q}}_{h,K} &= \{\mathbf{q}_h\} + C_{\mathbf{q}u} \llbracket u_h \rrbracket + C_{\mathbf{q}\mathbf{q}} \llbracket \mathbf{q}_h \rrbracket, \\ \widehat{u}_{h,K} &= \{u_h\} - C_{\mathbf{q}\mathbf{q}} \cdot \llbracket \mathbf{q}_h \rrbracket, \end{aligned}$$

and on its boundary, we take

$$\widehat{\mathbf{q}}_{h,K} := \begin{cases} \mathbf{q}_h^+ - C_{\mathbf{q}u}(u_h^+ - 0) \mathbf{n} & \text{on } \partial\Omega_{\mathcal{D}}, \\ \mathbf{g}_{\mathcal{N}} & \text{on } \partial\Omega_{\mathcal{N}}, \end{cases} \quad \widehat{u}_{h,K} := \begin{cases} 0 & \text{on } \partial\Omega_{\mathcal{D}}, \\ u_h^+ & \text{on } \partial\Omega_{\mathcal{N}}. \end{cases}$$

Note that the fact that the numerical trace $\widehat{u}_{h,K}$ does not depend on \mathbf{q}_h allows for an element-by-element elimination of the variable \mathbf{q}_h from the equations. This property justifies the name given to the LDG method.

Next, we show that LDG method is in fact a stabilized mixed finite element method. To see this, let us begin by noting that the DG approximate solution (\mathbf{q}_h, u_h) can also be characterized as the solution of

$$\begin{aligned} a(\mathbf{q}_h, \mathbf{v}) + b(u_h, \mathbf{v}) &= 0, \\ -b(w, \mathbf{q}_w) + c(u_h, w) &= F(w), \end{aligned}$$

for all $(\mathbf{v}, w) \in \mathcal{Q}_h \times \mathcal{U}_h$ where

$$\mathcal{Q}_h = \{\mathbf{v} : \mathbf{v} \in \mathcal{Q}(K) \forall K \in \mathcal{T}_h\}, \quad \mathcal{U}_h = \{w : w \in \mathcal{U}(K) \forall K \in \mathcal{T}_h\},$$

and

$$\begin{aligned} a(\mathbf{q}, \mathbf{r}) &:= \int_{\Omega} \mathbf{q} \cdot \mathbf{r} \, dx, \\ b(u, \mathbf{r}) &:= \sum_{K \in \mathcal{T}} \int_K u \nabla \cdot \mathbf{r} \, dx - \int_{\mathcal{E}_i} (\{u\} + C_{\mathbf{q}\mathbf{q}} \cdot \llbracket u \rrbracket) \llbracket \mathbf{r} \rrbracket \, ds, \\ c(u, v) &:= \int_{\mathcal{E}_{ih}} C_{\mathbf{q}u} \llbracket u \rrbracket \cdot \llbracket v \rrbracket \, ds + \int_{\partial\Omega} C_{\mathbf{q}u} uv \, ds, \\ F(\mathbf{r}) &:= \int_{\Omega} f v \, dx. \end{aligned}$$

It is well known that for the exact solution $(\mathbf{q} = \nabla u, u)$, we have the identity,

$$a(\mathbf{q}, \mathbf{q}) = F(u),$$

from which an H^1 -a priori estimate can be easily obtained. For the approximate solution of the DG method, we have instead,

$$a(\mathbf{q}_h, \mathbf{q}_h) + c(u_h, u_h) = F(u_h).$$

This shows that the stability of the DG method is enhanced by the jumps across inter-element boundaries since

$$c(u, v) := \int_{\mathcal{E}_{ih}} C_{\mathbf{q}u} |\llbracket u_h \rrbracket|^2 \, ds + \int_{\partial\Omega} C_{\mathbf{q}u} u_h^2 \, ds.$$

This also shows that the role of the coefficient $C_{\mathbf{q}u}$ is to control the amount of dissipation in the method. As we can see, this coefficient can also be considered to be a penalty coefficient for the jumps. The role of the other coefficient $C_{\mathbf{q}\mathbf{q}}$ is to maximize the sparsity of the matrices and to improve the accuracy of the method; see Cockburn et al. (2001).

Also in this framework, the jumps across inter-element boundaries are related to the local residual in a linear way; this shows that these methods are stabilized mixed methods. To see this, consider the local residuals

$$\mathbf{R}_1 = \mathbf{q}_h - \nabla u_h, \quad \text{and} \quad R_2 = -\nabla \cdot \mathbf{q}_h - f,$$

and use the weak formulation of the DG method and the definition of its numerical trace to get

$$\begin{aligned}\int_K \mathbf{R}_1 \cdot \mathbf{v} \, dx &= \int_{\partial K} \left(\left(-\frac{1}{2} \mathbf{n} - C_{\mathbf{q}\mathbf{q}} \right) \cdot \llbracket u_h \rrbracket \right) \mathbf{v} \cdot \mathbf{n} \, ds, \\ \int_K R_2 w \, dx &= \int_{\partial K} \left(\left(-\frac{1}{2} \mathbf{n} + C_{\mathbf{q}\mathbf{q}} \llbracket \mathbf{q}_h \rrbracket + C_{\mathbf{q}u} \llbracket u_h \rrbracket \right) \cdot \mathbf{n} \right) w \, ds,\end{aligned}$$

for all $(\mathbf{v}, w) \in \mathcal{Q}(K) \times \mathcal{U}(K)$.

Finally, let us show that to guarantee the existence and uniqueness of the approximate solution of the DG methods, the parameter $C_{\mathbf{q}u}$ has to be greater than zero and the local spaces $\mathcal{U}(K)$ and $\mathcal{Q}(K)$ must satisfy the following *compatibility* condition:

$$u_h \in \mathcal{U}(K) : \int_K \nabla u_h \cdot \mathbf{v} \, dx = 0 \quad \forall \mathbf{v} \in \mathcal{Q}(K) \quad \text{then} \quad \nabla u_h = \mathbf{0}.$$

This very simple, local condition implies a global inf-sup condition for the DG methods which, in fact, is extremely easy to prove due to the stability-enhancing effect of the inter-element jumps.

The approximate solution is well defined if and only if, the only approximate solution to the problem with $f = 0$ is the trivial solution. In that case, our stability identity gives

$$a(\mathbf{q}_h, \mathbf{q}_h) + c(u_h, u_h) = 0,$$

which implies that $\mathbf{q}_h = 0$, $\llbracket u_h \rrbracket = 0$ on \mathcal{E}_{ih} and $u_h = 0$ on $\partial\Omega$, provided that $C_{\mathbf{q}u} > 0$. We can now rewrite the first equation defining the method as follows:

$$\int_K \nabla u_h \cdot \mathbf{v} \, dx = 0, \quad \forall \mathbf{v} \in \mathcal{Q}_h,$$

which, by the compatibility condition, implies that $\nabla u_h = \mathbf{0}$. Hence $u_h = 0$, as required.

Other examples of DG methods are obtained by choosing their numerical traces as we can see in Table VI. There, the symbol $\alpha^r(\llbracket u_h \rrbracket)$ is used to denote a stabilization introduced by Bassi et al. (1997) and later studied by Brezzi et al. (2000). Its effect on the DG method is equivalent to the one produced by $C_{\mathbf{q}u} \llbracket u_h \rrbracket$; however, it produces a more sparse stiffness matrix. Not all DG methods were originally proposed in the mixed form we have used. Many of them were proposed directly in the primal form

$$B_h(u_h, v) = \int_{\Omega} f v.$$

The two main examples are the interior penalty (IP) method, proposed by Douglas, Jr. and Dupont (1976), for which we have

$$B_h(u_h, v) = \sum_K \int_K \nabla u_h \cdot \nabla v \, dx - \sum_e \int_e (\llbracket u_h \rrbracket \cdot \{\nabla_h v\} + \llbracket u_h \rrbracket \cdot \{\nabla_h v\}) \, ds + \sum_e \int_e \frac{\eta_0}{h} \llbracket u_h \rrbracket \cdot \llbracket v \rrbracket \, ds,$$

and the method proposed by Baumann and Oden (1999), for which we have

$$B_h(w, v) = \sum_K \int_K \nabla u_h \cdot \nabla v \, dx - \sum_e \int_e (\llbracket u_h \rrbracket \cdot \{\nabla_h v\} - \llbracket u_h \rrbracket \cdot \{\nabla_h v\}) \, ds.$$

A theoretical study of the DG methods for the elliptic model problem is carried out in a single, unified approach by Arnold et al. (2001). There, the mixed formulation is not used to carry out the analysis. Instead, the variable \mathbf{q}_h is eliminated from the equations. A primal formulation is thus obtained which is used to analyze the method. In Table VII we have summarized the properties of various DG methods. We display the properties of consistency and conservativity of the numerical fluxes, of stability of the method, of the type of stability (the symbol α^j is used to denote the stabilization associated with the terms $C_{\mathbf{q}u} \llbracket u_h \rrbracket^2$), the condition on $C_{\mathbf{q}u}$ for achieving stability, and the corresponding rates of convergence.

Castillo (2002) made a study of the condition number of various DG methods and compared them numerically. He found, in particular, that \mathbf{q}_h is a much better approximation to \mathbf{q} than ∇u_h ; that the penalization parameter $C_{\mathbf{q}u}$ must be taken as η_0/h , where h is a measure of the diameters of the elements, to obtain a condition number of the matrix for u_h of order h^{-2} ; and that when η_0 is taken to be too big, all the DG methods give similar approximations.

How to couple DG methods with the classical conforming methods was shown by Alotto et al. (2001) and Perugia and Schötzau (2001). Moreover, Perugia and Schötzau (2001) combined the theoretical framework developed by Arnold et al. (2001) with the techniques of analysis of non-conforming methods to obtain optimal error estimates for the resulting coupling. How to couple DG methods with mixed methods was shown by Cockburn and Dawson (2002).

Table VI. Some DG methods and their numerical fluxes. Taken from Arnold et al. (2001) and slightly modified.

Method	$\hat{\mathbf{q}}_{e,K}$	$\hat{u}_{h,K}$
Bassi and Rebay (1997a)	$\{\mathbf{q}_h\}$	$\{u_h\}$
Cockburn and Shu (1998a)	$\{\mathbf{q}_h\} + C_{\mathbf{q}u} \llbracket u_h \rrbracket - C_{\mathbf{q}\mathbf{q}} \llbracket \mathbf{q}_h \rrbracket$	$\{u_h\} + C_{\mathbf{q}\mathbf{q}} \cdot \llbracket u_h \rrbracket$
Castillo et al. (2000)	$\{\mathbf{q}_h\} + C_{\mathbf{q}u} \llbracket u_h \rrbracket - C_{\mathbf{q}\mathbf{q}} \llbracket \mathbf{q}_h \rrbracket$	$\{u_h\} + C_{\mathbf{q}\mathbf{q}} \cdot \llbracket u_h \rrbracket + C_{u\mathbf{q}} \llbracket \mathbf{q}_h \rrbracket$
Brezzi et al. (2000)	$\{\mathbf{q}_h\} - \alpha^r(\llbracket u_h \rrbracket)$	$\{u_h\}$
Douglas, Jr. and Dupont (1976)	$\{\nabla u_h\} + C_{\mathbf{q}u} \llbracket u_h \rrbracket$	$\{u_h\}$
Bassi et al. (1997)	$\{\nabla u_h\} - \alpha^r(\llbracket u_h \rrbracket)$	$\{u_h\}$
Baumann and Oden (1999)	$\{\nabla u_h\}$	$\{u_h\} - \mathbf{n}_K \cdot \llbracket u_h \rrbracket$
Rivière et al. (1999)	$\{\nabla u_h\} + C_{\mathbf{q}u} \llbracket u_h \rrbracket$	$\{u_h\} - \mathbf{n}_K \cdot \llbracket u_h \rrbracket$
Babuška and Zlámal (1973)	$C_{\mathbf{q}u} \llbracket u_h \rrbracket$	$u_h _K$
Brezzi et al. (2000)	$-\alpha^r(\llbracket u_h \rrbracket)$	$u_h _K$

4.2. Solvers

Solvers specifically designed for the linear system of equations given by DG methods have started to be developed. For the time-dependent compressible Navier-Stokes, Bassi and Rebay (2000) experimented with the preconditioned GMRES and found that the simple block-Jacobi pre-conditioning was the most efficient. Feng and Karakashian (2001) studied a domain decomposition preconditioner for DG approximations for purely elliptic problems.

Table VII. Properties of the DG methods. Taken from Arnold et al. (2001) and slightly modified.

Method	consis.	conserv.	stab.	type	$\eta_0 = h C_{qu}$	H^1	L^2
Brezzi et al. (1999)	✓	✓	✓	α^r	$\eta_0 > 0$	h^p	h^{p+1}
Cockburn and Shu (1998a)	✓	✓	✓	α^j	$\eta_0 > 0$	h^p	h^{p+1}
Castillo et al. (2000)	✓	✓	✓	α^j	$\eta_0 > 0$	h^p	h^{p+1}
Douglas, Jr. and Dupont (1976)	✓	✓	✓	α^j	$\eta_0 > \eta^*$	h^p	h^{p+1}
Bassi et al. (1997)	✓	✓	✓	α^r	$\eta_0 > 3$	h^p	h^{p+1}
Rivière et al. (1999)	✓	×	✓	α^j	$\eta_0 > 0$	h^p	h^p
Babuška and Zlámal (1973)	×	×	✓	α^j	$\eta_0 \approx h^{-2p}$	h^p	h^{p+1}
Brezzi et al. (2000)	×	×	✓	α^r	$\eta_0 \approx h^{-2p}$	h^p	h^{p+1}
Baumann and Oden (1999) ($p = 1$)	✓	×	×	-	-	×	×
Baumann and Oden (1999) ($p \geq 2$)	✓	×	×	-	-	h^p	h^p
Bassi and Rebay (1997a)	✓	✓	×	-	-	$[h^p]$	$[h^{p+1}]$

The condition number of their non-overlapping preconditioner grows linearly with the number of degrees of freedom in each sub-domain. Later, Lasser and Toselli (2000) found an overlapping domain decomposition method for DG methods for linear advection-diffusion problems whose condition number is independent of the number of degrees of freedom and the number of subdomains. Another significant result has been obtained by Gopalakrishnan and Kanschat (2003b) who devised a multigrid method for solving the matrix equation of the Interior Penalty method for elliptic problems. They proved that it convergences in a fixed number of iterations; they have also devised a method for the steady-state convection-diffusion problem which converges with a fixed number of iterations independently of the size of the convection coefficients. These solvers were generalized to the LDG method in primal form, the method by Bassi and Rebay (1997a) and the method by Brezzi et al. (1999) by Gopalakrishnan and Kanschat (2003a). Based on these solvers, preconditioners for the LDG saddle point systems arising from the mixed discretization of Poisson and Stokes equations were introduced by Kanschat (2003).

5. DG methods for convection-dominated problems

In this section, we consider the application of the DG method to various problems in fluid dynamics in which convection plays a dominant role. They include the shallow water equations and the equations of incompressible and compressible fluid flow.

5.1. Convection-diffusion problems

In this subsection, we consider the LDG methods for the following convection-diffusion model problem

$$u_t + \nabla \cdot (f(u) - a(u)\nabla u) = 0 \quad \text{in } \Omega \times (0, T), \quad u(x, 0) = u_0(x) \quad \forall x \in \Omega.$$

To define a DG method, we first notice that, since the matrix $a(u)$ is assumed to be symmetric and semi-positive definite, there exists a symmetric matrix $b(u)$ such that $a = b^2$. This allows us to introduce the auxiliary variable $\mathbf{q} = b\nabla u$, and rewrite the model problem as follows:

$$\begin{aligned} u_t + \nabla \cdot f(u) - \nabla \cdot (b(u)\mathbf{q}) &= 0 & \text{in } \Omega \times (0, T), \\ q_i &= \nabla \cdot \mathbf{g}_i(u) & \text{in } \Omega \times (0, T), \quad 1 \leq i \leq N, \\ u(x, 0) &= u_0(x) & \forall x \in \Omega, \end{aligned}$$

where q_i is the i -th component of the vector \mathbf{q} , and $\mathbf{g}_i(u)$ is the vector whose j -th component is $\int^u b_{ji}(s) ds$. A DG method is now obtained in a most straightforward way. For details, see Cockburn and Shu (1998a) and Cockburn and Dawson (2000).

Let us give a computational result of the application of the LDG method to the two-dimensional flow and transport in shallow water from the paper by Aizinger and Dawson (2003). The system of shallow water equations can be written as

$$\mathbf{c}_t + \nabla \cdot (\mathbf{A} + (D\nabla)\mathbf{c}) = \mathbf{h}(\mathbf{c}),$$

where $\mathbf{c}^t = (\xi, u, v)$; here, ξ is the deflection of the air-water interface from the mean sea level, and (u, v) is the depth-averaged horizontal velocity. For details about the remaining terms, see Aizinger and Dawson (2003). What is relevant for our purposes is that the above is a non-linear convection-diffusion-reaction equation which can be easily discretized by the LDG method. In Fig. 29, we see a mesh (top) of 14,269 triangles, highly graded towards the coast, and the function ξ (bottom) computed for a high inflow of $35,000m^3/s$ for the Mississippi River; an open sea boundary condition is assumed. In comparison with the no-inflow situation (not shown here), the elevation increases about half a foot near the lower Louisiana coast.

5.1.1. Incompressible flow Next, let us consider the Oseen equations of incompressible fluid flow, namely,

$$\begin{aligned} -\nu\Delta\mathbf{u} + (\boldsymbol{\beta} \cdot \nabla)\mathbf{u} + \gamma\mathbf{u} + \nabla p &= \mathbf{f} & \text{in } \Omega, \\ \nabla \cdot \mathbf{u} &= 0 & \text{in } \Omega, \\ \mathbf{u} &= \mathbf{g} & \text{on } \Gamma, \end{aligned}$$

where \mathbf{u} is the velocity, p the pressure, $\mathbf{f} \in L^2(\Omega)^2$ a prescribed external body force, $\nu > 0$ the kinematic viscosity, $\boldsymbol{\beta}$ a convective velocity field and γ a given scalar function. As usual, we take Ω to be a bounded domain of \mathbb{R}^2 with boundary $\Gamma = \partial\Omega$, and the Dirichlet datum

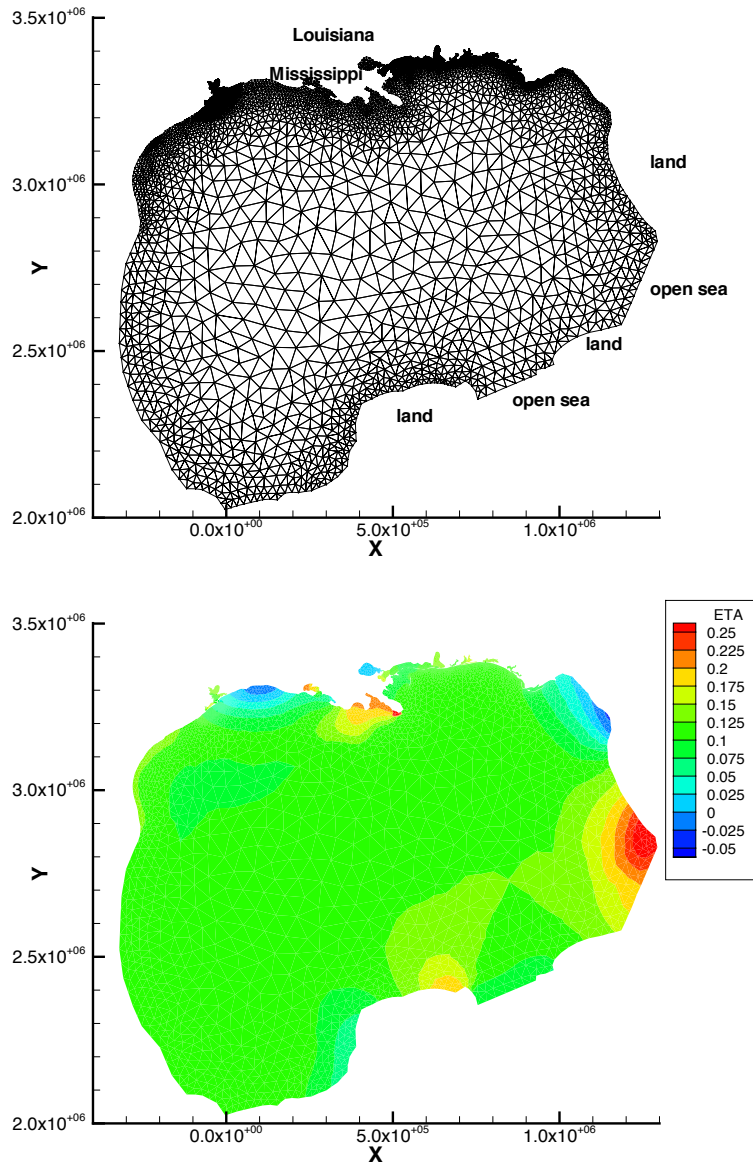


Figure 29. Gulf of Mexico mesh (top) and surface elevation for high inflow of the Mississippi river (bottom). From Aizinger and Dawson (2003).

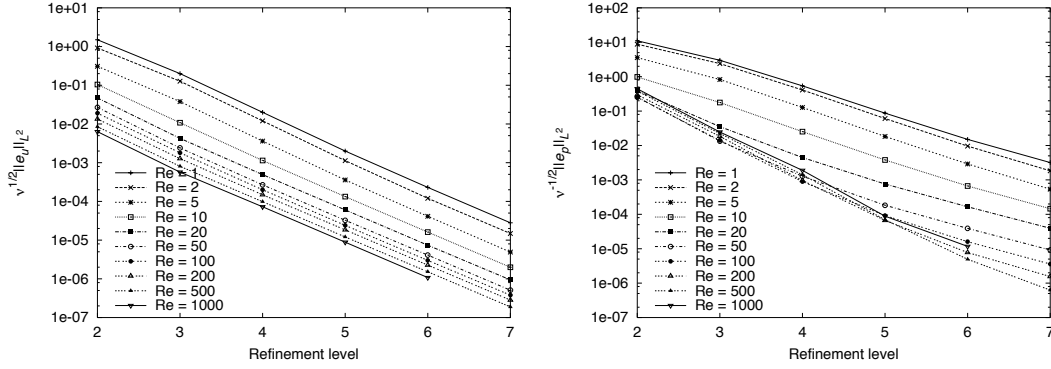


Figure 30. Scaled L^2 -errors in \mathbf{u} and p with bilinear approximations for different Reynolds numbers. From Cockburn et al. (2002).

$\mathbf{g} \in H^{1/2}(\Gamma)^2$ to satisfy the compatibility condition $\int_{\Gamma} \mathbf{g} \cdot \mathbf{n} \, ds = 0$, where \mathbf{n} denotes the unit outward normal vector to Γ . We also assume that

$$\gamma(\mathbf{x}) - \frac{1}{2} \nabla \cdot \boldsymbol{\beta}(\mathbf{x}) =: \gamma_0(\mathbf{x}) \geq 0, \quad \mathbf{x} \in \Omega. \quad (12)$$

This condition guarantees the existence and uniqueness of a solution $(\mathbf{u}, p) \in H_g^1(\Omega)^2 \times L_0^2(\Omega)$ where $H_g^1(\Omega)^2 := \{\mathbf{u} \in H^1(\Omega)^2 : \mathbf{u}|_{\Gamma} = \mathbf{g}\}$ and $L_0^2(\Omega) := \{p \in L^2(\Omega) : \int_{\Omega} p \, dx = 0\}$.

In Fig. 30, we display the norms of the error in the velocity and the pressure for the LDG method as a function of the mesh size for several Reynolds numbers for the so-called Kovasznay flow. Bi-quadratic approximations on squares are used. The norms are scaled with the appropriate powers of ν so as to make all the quantities dimensionally equivalent - see Cockburn et al. (2002) for details. We can see that the convergence of the above errors is not altered as the Reynolds number varies from 1 to 1,000 which confirms the expected robustness of the LDG method with respect to an increase in the strength of the convection.

5.1.2. Compressible fluid flow Finally, we present some numerical results for the compressible Navier-Stokes equations,

$$\begin{aligned} \rho_t + (\rho v_j)_{,j} &= 0, \\ (\rho v_i)_t + (\rho v_i v_j - \sigma_{ij})_{,j} &= f_i, \\ (\rho e)_t + (\rho e v_j - \sigma_{ij} v_i + q_i)_{,j} &= f_i v_i, \end{aligned}$$

where ρ is the density, v the velocity, e the internal energy, and f the external body forces. The viscous stress σ and the heat flux q are given by

$$\begin{aligned} \sigma_{ij} &= (-p + \lambda v_{i,i}) \delta_{ij} + \mu (v_{i,j} + v_{j,i}), \\ q_i &= -\kappa T_{,i}, \end{aligned}$$

where p is the pressure and T the temperature.

In Fig. 31, we show a steady-state calculation of the laminar Mach 0.8 flow around a NACA 0012 airfoil with Reynolds number 73. No limiter was applied.

Our last example is a time-dependent computation of the flow around a cylinder in two space dimensions. The Reynolds number is 10,000 and the Mach number 0.2. In Fig. 32, we see the detail of a mesh of 680 triangles (with curved sides fitting the cylinder) and polynomials whose degree could vary from element to element; the maximum degree was 5. Note how the method is able to capture the shear layer instability observed experimentally. For more details, see Lomtev and Karniadakis (1999).

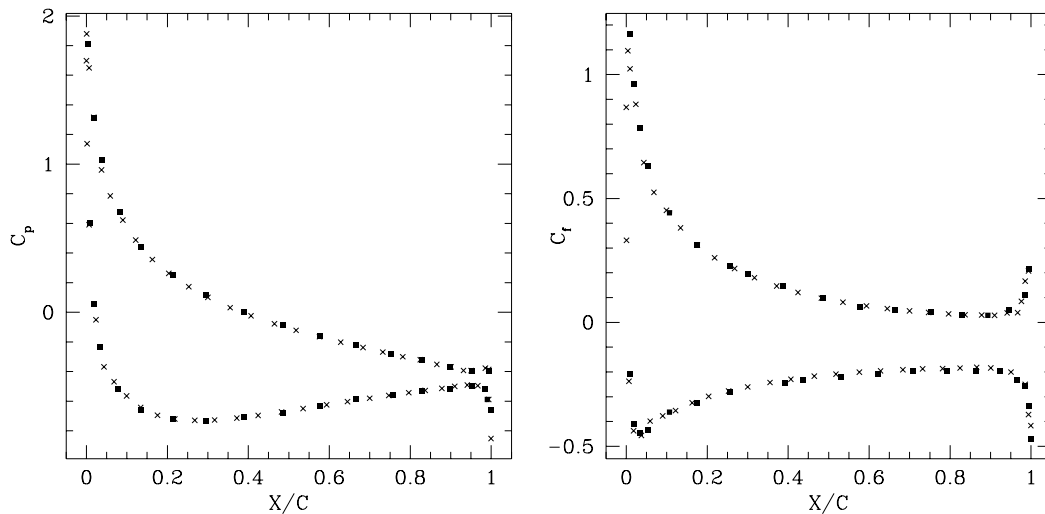


Figure 31. Pressure (left) and drag (right) coefficient distributions. The squares were obtained by with cubics by Bassi and Rebay (1997a) and the crosses by with polynomials of degree 6 by Lomtev and Karniadakis (1999).

6. Concluding remarks and bibliographical notes

In this paper, we have studied the DG method for computational fluid dynamics. Most of the material in this article has been taken from the short, introductory monograph by Cockburn (1999), from the review by Cockburn and Shu (2001), and from the recent paper (written for a very wide audience) by Cockburn (2003b). The reader interested in a history of the development of DG methods and in the state of the art up to 1999 is referred to Cockburn et al. (2000).

The set of references in this paper was not meant to be exhaustive, and several important topics were left without being properly considered or emphasized for considerations of space.

One such topic is the very important issue of adaptivity for DG methods. For adaptivity on linear, steady-state hyperbolic problems, the reader is referred to the papers by Bey (1994), Bey and Oden (1996), and then to the papers Houston et al. (2000), Houston et al. (2001), Houston and Süli (2001), Houston et al. (2002), and Süli and Houston (2002). For adaptivity for non-linear problems (and a different approach), see the papers by Biswas et al. (1994),

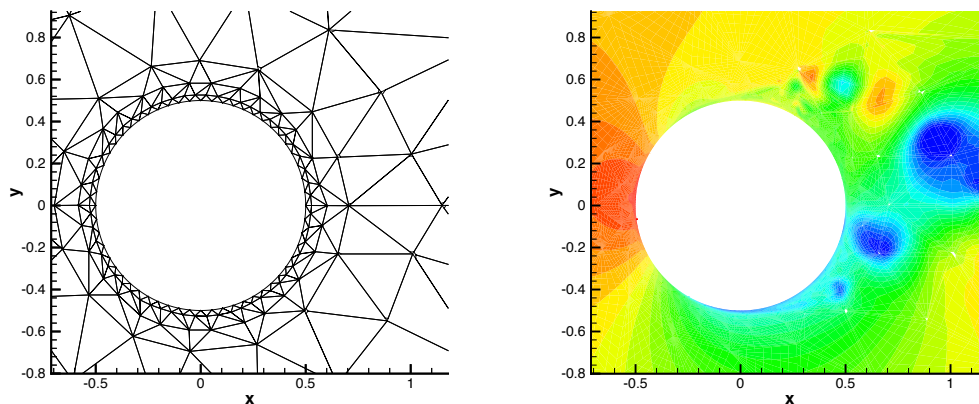


Figure 32. Flow around a cylinder with Reynolds number 10,000 and Mach number 0.2. Detail of the mesh (top) and density (bottom) around the cylinder. From Lomtev and Karniadakis (1999).

Devine et al. (1995), Devine and Flaherty (1996), Flaherty et al. (1997), Flaherty et al. (1998), Flaherty et al. (1999), Flaherty et al. (2000). For a posteriori error estimation for second-order elliptic problems, see the papers by Becker et al. (2003) and by Karakashian and Pascal (2003) for estimates of the energy norm; see the paper by Rivière and Wheeler (2002) for an estimate of the L^2 -norm.

Another topic is the issue of coupling DG methods with other methods. Besides the papers already mentioned in the section on DG methods for elliptic equations, we must add the papers by Dawson and Proft (2002) and Dawson and Proft (2003), devoted to the discontinuous and coupled continuous/discontinuous Galerkin methods for the shallow water equations. This effort is very important, as it is based on the idea of using different schemes in different parts of the computational domain in order to fully exploit their individual virtues. This will not only produce more efficient codes, but will also facilitate the handling of multi-physics models.

Yet another is the issue of dealing with constraints like the divergence-free condition for incompressible fluid flow. This condition has been imposed inside each element by Baker et al. (1990), Karakashian and Jureidini (1998), and Karakashian and Katsaounis (2000). However, the issue has not been addressed in the many papers on DG methods for incompressible fluid flow.

To end, let us point out that these days, the field is rapidly evolving and that several new developments are already taking place. This is particularly true for super-convergence results (see, for example, the papers by Adjrid and Massey (2002) and by Krivodonova and Flaherty (2001)) slope limiters, space-time DG methods, and local time-stepping methods for explicit DG methods (see the paper by Remacle et al. (2001)).

ACKNOWLEDGEMENTS

The author would like to thank Thomas Hughes for the kind invitation to write this paper. He would

also like to thank the many colleagues that provided most of the figures in this paper: Francesco Bassi, Paul Castillo, Nicolas Chauvegeon, Clint Dawson, Paul Houston, Igor Lomtev, Guido Kanschat, George Karniadakis, Manoj Prasad, Stefano Rebay, Chi-Wang Shu, Jaap van der Vegt and Harmen van der Ven. Thanks are also due to Paul Houston for a careful reading of the paper. Finally, the author would like to thank Clint Dawson, Guido Kanschat, Paul Houston, Dominik Schötzau and Harmen van der Ven for useful feedback on the first version of the manuscript.

REFERENCES

- S. Adjerid and T.C. Massey (2002). A posteriori discontinuous finite element error estimation for two-dimensional hyperbolic problems. *Comput. Methods Appl. Mech. Engrg.*, 191:5877–5897.
- V. Aizinger and C.N. Dawson (2003). A Discontinuous Galerkin Method for two-dimensional flow and transport in shallow water. Technical Report 03-16, TICAM.
- V. Aizinger, C.N. Dawson, B. Cockburn and P. Castillo (2000). Local discontinuous Galerkin method for contaminant transport. *Advances in Water Resources*, 24:73–87.
- P. Alotto, A. Bertoni, I. Perugia and D. Schötzau (2001). Discontinuous Finite Element Methods for the Simulation of Rotating Electrical Machines. *COMPEL*, 20:448–462.
- D.N. Arnold, F. Brezzi, B. Cockburn and D. Marini (2001). Unified analysis of discontinuous Galerkin methods for elliptic problems. *SIAM J. Numer. Anal.*, 39:1749–1779.
- H.L. Atkins and C.-W. Shu (1998). Quadrature-free implementation of discontinuous Galerkin methods for hyperbolic equations. *AIAA Journal*, 36.
- I. Babuška and M. Zlámal (1973). Nonconforming elements in the finite element method with penalty. *SIAM J. Numer. Anal.*, 10:863–875.
- G.A. Baker, W.N. Jureidini and O. A. Karakashian (1990). Piecewise solenoidal vector fields and the Stokes problem. *SIAM J. Numer. Anal.*, 27:1466–1485.
- T. Barth (2000). Simplified DG methods for systems of conservation laws with convex extension. In Cockburn, B., Karniadakis, G., and Shu, C.-W., editors, *Discontinuous Galerkin Methods. Theory, Computation and Applications*, volume 11 of *Lecture Notes in Computational Science and Engineering*, pages 63–75, Berlin. Springer Verlag.
- F. Bassi and S. Rebay (1997a). A high-order accurate discontinuous finite element method for the numerical solution of the compressible Navier-Stokes equations. *J. Comput. Phys.*, 131:267–279.
- F. Bassi and S. Rebay (1997b). High-order accurate discontinuous finite element solution of the 2D Euler equations. *J. Comput. Phys.*, 138:251–285.
- F. Bassi and S. Rebay (2000). GMRES for discontinuous Galerkin solution of the compressible Navier-Stokes equations. In Cockburn, B., Karniadakis, G., and Shu, C.-W., editors, *Discontinuous Galerkin Methods. Theory, Computation and Applications*, volume 11 of *Lecture Notes in Computational Science and Engineering*, pages 197–208, Berlin. Springer Verlag.
- Bassi, F., Rebay, S., Mariotti, G., Pedinotti, S. and Savini, M. (1997). A High-Order Accurate Discontinuous Finite Element Method for Inviscid and Viscous Turbomachinery Flows. In Decuyper, R. and Dibelius, G., editors, *2nd European Conference on Turbomachinery Fluid Dynamics and Thermodynamics*, pages 99–108, Antwerpen, Belgium. Technologisch Instituut.
- C.E. Baumann and J.T. Oden (1999). A discontinuous *hp*-finite element method for convection-diffusion problems. *Comput. Methods Appl. Mech. Engrg.*, 175:311–341.
- R. Becker, P. Hansbo and M. G. Larson (2003). Energy norm a posteriori error estimation for discontinuous Galerkin methods. *Comput. Methods Appl. Mech. Engrg.*, 192:723–733.
- K.S. Bey (1994). *An hp-adaptive discontinuous Galerkin method for hyperbolic conservation laws*. PhD thesis, The University of Texas at Austin.

- K.S. Bey and J.T. Oden (1996). *hp*-version discontinuous Galerkin methods for hyperbolic conservation laws. *Comput. Methods Appl. Mech. Engrg.*, 133:259–286.
- R. Biswas, K.D. Devine and J. Flaherty (1994). Parallel, adaptive finite element methods for conservation laws. *Appl. Numer. Math.*, 14:255–283.
- O.J. Boelens, H. van der Ven, B. Oskam and A.A. Hassan (2002). The boundary conforming discontinuous Galerkin finite element approach for rotorcraft simulations. *J. of Aircraft*, 39:776–785.
- F. Brezzi, G. Manzini, D. Marini, P. Pietra and A. Russo (1999). Discontinuous finite elements for diffusion problems. In *Atti Convegno in onore di F. Brioschi (Milano 1997)*, pages 197–217. Istituto Lombardo, Accademia di Scienze e Lettere.
- F. Brezzi, G. Manzini, D. Marini, P. Pietra and A. Russo (2000). Discontinuous Galerkin Approximations for elliptic Problems. *Numerical Methods for Partial Differential Equations*, 16:365–378.
- A. Burbeau, P. Sagaut and Ch.-H. Bruneau (2001). A problem-independent limiter for high-order Runge-Kutta discontinuous Galerkin methods. *J. Comput. Phys.*, 169:111–150.
- P. Castillo (2002). Performance of discontinuous Galerkin methods for elliptic PDE's. *SIAM J. Math. Anal.*, 24:524–5547.
- P. Castillo, B. Cockburn, I. Perugia and D. Schötzau (2000). An a priori error analysis of the local discontinuous Galerkin method for elliptic problems. *SIAM J. Numer. Anal.*, 38:1676–1706.
- B. Cockburn (1999). Discontinuous Galerkin Methods for Convection-Dominated Problems. In Barth, T. and Deconink, H., editors, *High-Order Methods for Computational Physics*, volume 9 of *Lecture Notes in Computational Science and Engineering*, pages 69–224. Springer Verlag, Berlin.
- B. Cockburn (2003a). Continuous dependence and error estimation for viscosity methods. *Acta Numerica*, 12.
- B. Cockburn (2003b). Discontinuous Galerkin Methods. *ZAMM Z. Angew. Math. Mech.* to appear.
- B. Cockburn and C. Dawson (2000). Some extensions of the local discontinuous Galerkin method for convection-diffusion equations in multidimensions. In Whiteman, J., editor, *The Proceedings of the Conference on the Mathematics of Finite Elements and Applications: MAFELAP X*, pages 225–238. Elsevier.
- B. Cockburn and C. Dawson (2002). Approximation of the velocity by coupling discontinuous Galerkin and mixed finite element methods for flow problems. *Comput. Geosci. (Special issue: Locally Conservative Numerical Methods for Flow in Porous Media)*, 6:502–522.
- B. Cockburn and P.-A. Gremaud (1996). Error estimates for finite element methods for nonlinear conservation laws. *SIAM J. Numer. Anal.*, 33:522–554.
- B. Cockburn, S. Hou and C.-W. Shu (1990). TVB Runge-Kutta Local Projection Discontinuous Galerkin Finite Element Method for Conservation Laws IV: The Multidimensional Case. *Math. Comp.*, 54:545–581.
- B. Cockburn, G. Kanschat, I. Perugia and D. Schötzau (2001). Superconvergence of the local discontinuous Galerkin method for elliptic problems on Cartesian grids. *SIAM J. Numer. Anal.*, 39:264–285.
- B. Cockburn, G. Kanschat and D. Schötzau (2002). Local discontinuous Galerkin methods for the Oseen equations. *Math. Comp.* to appear.
- B. Cockburn, G.E. Karniadakis and C.-W. Shu (2000). The development of discontinuous Galerkin methods. In Cockburn, B., Karniadakis, G., and Shu, C.-W., editors, *Discontinuous Galerkin Methods. Theory, Computation and Applications*, volume 11 of *Lecture Notes in Computational Science and Engineering*, pages 3–50, Berlin. Springer Verlag.
- B. Cockburn, M. Luskin, C.-W. Shu and E. Süli (2003). Enhanced accuracy by post-processing for finite element methods for hyperbolic equations. *Math. Comp.*, 72:577–606 (electronic).

- B. Cockburn and C.-W. Shu (1998a). The local Discontinuous Galerkin Method for time-dependent convection-diffusion systems. *SIAM J. Numer. Anal.*, 35:2440–2463.
- B. Cockburn and C.-W. Shu (1998b). The Runge-Kutta Discontinuous Galerkin Finite Element Method for Conservation Laws V: Multidimensional Systems. *J. Comput. Phys.*, 141:199–224.
- B. Cockburn and C.-W. Shu (2001). Runge-Kutta Discontinuous Galerkin Methods for convection-dominated problems. *J. Sci. Comput.*, 16:173–261.
- C. Dawson and J. Proft (2002). Discontinuous and coupled continuous/discontinuous Galerkin methods for the shallow water equations. *Comput. Methods Appl. Mech. Engrg.*, 191:4721–4746.
- C. Dawson and J. Proft (2003). Discontinuous/continuous Galerkin methods for coupling the primitive and wave continuity equations of shallow water, *Comput. Methods Appl. Mech. Engrg.*, to appear.
- K.D. Devine and J.E. Flaherty (1996). Parallel adaptive *hp*-refinement techniques for conservation laws. *Appl. Numer. Math.*, 20:367–386.
- K.D. Devine, J.E. Flaherty, R.M. Loy and S.R. Wheat (1995). Parallel partitioning strategies for the adaptive solution of conservation laws. In Babuška, I., Flaherty, J., Henshaw, W., Hopcroft, J., Olinger, J., and Tezduyar, T., editors, *Modeling, mesh generation, and adaptive numerical methods for partial differential equations*, volume 75 of *The IMA Volumes in Mathematics and its Applications*, pages 215–242, New York, New York. Springer-Verlag.
- J. Douglas, Jr. and T. Dupont (1976). *Interior penalty procedures for elliptic and parabolic Galerkin methods*, volume 58 of *Lecture Notes in Physics*. Springer-Verlag, Berlin.
- M. Dubiner (1991). Spectral Methods on Triangles and Other Domains. *J. Sci. Comp.*, 6:345–390.
- R.S. Falk and G.R. Richter (1999). Explicit finite element methods for symmetric hyperbolic equations. *SIAM J. Numer. Anal.*, 36:935–952.
- X. Feng and O. A. Karakashian (2001). Two-level non-overlapping Schwarz methods for a discontinuous Galerkin method. *SIAM J. Numer. Anal.*, 39:1343–1365 (electronic).
- J.E. Flaherty, R.M. Loy, C. Özturan, M.S. Shephard, B.K. Szymanski, J.D. Teresco and L.H. Ziantz (1998). Parallel Structures and Dynamic Load Balancing for Adaptive Finite Element Computation. *Appl. Numer. Math.*, 26:241–265.
- J.E. Flaherty, R.M. Loy, M.S. Shephard, M.L. Simone, B.K. Szymanski, J.D. Teresco and L.H. Ziantz (1999). Distributed Octree Data Structures and Local Refinement Method for the Parallel Solution of Three-Dimensional Conservation Laws. In Bern, M., Flaherty, J., and Luskin, M., editors, *Grid Generation and Adaptive Algorithms*, volume 113 of *The IMA Volumes in Mathematics and its Applications*, pages 113–134, Minneapolis. Institute for Mathematics and its Applications, Springer.
- J.E. Flaherty, R.M. Loy, M.S. Shephard, B.K. Szymanski, J.D. Teresco and L.H. Ziantz (1997). Adaptive local refinement with octree load-balancing for the parallel solution of three-dimensional conservation laws. *J. Parallel and Dist. Comput.*, 47:139–152.
- J. Flaherty, R. Loy, M.S. Shephard and J. Teresco (2000). Software for the parallel adaptive solution of conservation laws by a discontinuous Galerkin method. In Cockburn, B., Karniadakis, G., and Shu, C.-W., editors, *Discontinuous Galerkin Methods. Theory, Computation and Applications*, volume 11 of *Lecture Notes in Computational Science and Engineering*, pages 113–123, Berlin. Springer Verlag.
- K.O. Friedrichs (1958). Symmetric positive linear differential equations. *Comm. Pure and Appl. Math.*, 11:333–418.
- J. Gopalakrishnan and G. Kanschat (2003a). Application of unified DG analysis to preconditioning DG methods. In *Proceedings of the Second M.I.T. Conference on Computational Fluid and Solid Mechanics, June 17 - 20*, (K. Bathe, editor), pages 1943–1945. Elsevier.
- J. Gopalakrishnan and G. Kanschat (2003b). A multilevel discontinuous Galerkin method. *Numer. Math.*, 95. to appear.

- S. Gottlieb and C.-W. Shu (1998). Total variation diminishing Runge-Kutta schemes. *Math. Comp.*, 67:73–85.
- S. Gottlieb, C.-W. Shu and E. Tadmor (2000). Strong stability preserving high order time discretization methods. *SIAM Rev.*, 43:89–112.
- K. Harriman and P. Houston and B. Senior and E. Süli. *hp*-Version Discontinuous Galerkin Methods with Interior Penalty for Partial Differential Equations with Nonnegative Characteristic Form. In C.-W. Shu, T. T. and Cheng, S.-Y., editors, *Proceedings of the International Conference on Scientific Computing and Partial Differential Equations*. AMS Contemporary Mathematics. to appear.
- R. Hartmann and P. Houston (2002a). Adaptive discontinuous Galerkin finite element methods for nonlinear hyperbolic conservation laws. *SIAM J. Sci. Comput.*, 24:979–1004 (electronic).
- R. Hartmann and P. Houston (2002b). Adaptive discontinuous Galerkin finite element methods for the compressible Euler equations. *J. Comput. Phys.*, 183:508–532.
- J.S. Hesthaven and T. Warburton (2002). Nodal high-order methods on unstructured grids. I. Time-domain solution of Maxwell’s equations. *J. Comput. Phys.*, 181:186–221.
- P. Houston, C. Schwab and E. Süli (2000). Stabilized *hp*-finite element methods for hyperbolic problems. *SIAM J. Numer. Anal.*, 37:1618–1643.
- P. Houston, C. Schwab and E. Süli (2001). *hp*-adaptive discontinuous Galerkin finite element methods for hyperbolic problems. *SIAM J. Math. Anal.*, 23:1226–1252.
- P. Houston, B. Senior and E. Süli (2002). *hp*-discontinuous Galerkin finite element methods for hyperbolic problems: error analysis and adaptivity. *Internat. J. Numer. Methods Fluids*, 40:153–169. ICFD Conference on Numerical Methods for Fluid Dynamics (Oxford, 2001).
- P. Houston and E. Süli (2001). *hp*-adaptive discontinuous Galerkin finite element methods for first-order hyperbolic problems. *SIAM J. Sci. Comput.*, 23:1226–1252 (electronic).
- J. Jaffré, C. Johnson and A. Szepessy (1995). Convergence of the discontinuous Galerkin finite element method for hyperbolic conservation laws. *Mathematical Models & Methods in Applied Sciences*, 5:367–386.
- G.-S. Jiang and C.-W. Shu (1994). On a cell entropy inequality for discontinuous Galerkin methods. *Math. Comp.*, 62:531–538.
- C. Johnson, U. Nävert and J. Pitkäranta (1984). Finite element methods for linear hyperbolic problems. *Comput. Methods Appl. Mech. Engrg.*, 45:285–312.
- C. Johnson and J. Pitkäranta (1986). An analysis of the discontinuous Galerkin method for a scalar hyperbolic equation. *Math. Comp.*, 46:1–26.
- G. Kanschat. Preconditioning Methods for local discontinuous Galerkin Discretizations. *SIAM J. Sci. Comp.* to appear.
- O. A. Karakashian and W.N. Jureidini (1998). A nonconforming finite element method for the stationary Navier-Stokes equations. *SIAM J. Numer. Anal.*, 35:93–120.
- O. A. Karakashian and T. Katsaounis (2000). A discontinuous Galerkin method for the incompressible Navier-Stokes equations. In Cockburn, B., Karniadakis, G., and Shu, C.-W., editors, *Discontinuous Galerkin Methods. Theory, Computation and Applications*, volume 11 of *Lecture Notes in Computational Science and Engineering*, pages 157–166, Berlin. Springer Verlag.
- O. A. Karakashian and F. Pascal (2003). A posteriori error estimates for a discontinuous Galerkin approximation of a second order elliptic problems. *SIAM J. Numer. Anal.* to appear.
- G.E. Karniadakis and S.J. Sherwin (1999). *Spectral/hp Element Methods in CFD*. Oxford University Press.
- D.S. Kershaw, M.K. Prasad, M.J. Shaw and J.L. Milovich (1998). 3D unstructured mesh ALE hydrodynamics with the upwind discontinuous Galerkin method. *Comput. Methods Appl. Mech. Engrg.*, 158:81–116.

- L. Krivodonova and J.E. Flaherty (2001). Error estimation for discontinuous Galerkin solutions of multidimensional hyperbolic problems. *Advances in Computational Mathematics*, submitted.
- C. Lasser and A. Toselli (2000). An overlapping domain decomposition preconditioner for a class of discontinuous Galerkin approximations of advection-diffusion problems. Technical Report 2000-12, Seminar für Angewandte Mathematik, ETH Zürich.
- P. Lesaint and P.A. Raviart (1974). On a finite element method for solving the neutron transport equation. In de Boor, C., editor, *Mathematical aspects of finite elements in partial differential equations*, pages 89–145. Academic Press.
- I. Lomtev and G.E. Karniadakis (1999). A discontinuous Galerkin method for the Navier-Stokes equations. *Int. J. Numer. Meth. Fluids*, 29:587–603.
- R.B. Lowrie (1996). *Compact higher-order numerical methods for hyperbolic conservation laws*. PhD thesis, University of Michigan.
- R. B. Lowrie, P. L. Roe and B. van Leer (1995). A Space-Time Discontinuous Galerkin Method for the Time-Accurate Numerical Solution of Hyperbolic Conservation Laws. In *Proceedings of the 12th AIAA Computational Fluid Dynamics Conference*. Paper 95-1658.
- R. B. Lowrie, P. L. Roe and B. van Leer (1998). Space-Time Methods for Hyperbolic Conservation Laws. In *Barriers and Challenges in Computational Fluid Dynamics*, volume 6 of *ICASE/LaRC Interdisciplinary Series in Science and Engineering*, pages 79–98. Kluwer.
- S. Osher (1984). Convergence of Generalized MUSCL Schemes. *SIAM J. Numer. Anal.*, 22:947–961.
- I. Perugia and D. Schötzau (2001). On the coupling of local discontinuous Galerkin and conforming finite element methods. *J. Sci. Comput.*, 16:411–433.
- T. Peterson (1991). A note on the convergence of the Discontinuous Galerkin method for a scalar hyperbolic equation. *SIAM J. Numer. Anal.*, 28:133–140.
- W.H. Reed and T.R. Hill (1973). Triangular mesh methods for the neutron transport equation. Technical Report LA-UR-73-479, Los Alamos Scientific Laboratory.
- J.-F. Remacle, X. Li, N. Chevaugeon, M. S. Shephard and J. E. Flaherty (2003). Anisotropic adaptive simulation of transient flows using discontinuous Galerkin methods. Submitted.
- J.-F. Remacle, K. Pinchedez, J.E. Flaherty and M.S. Shephard (2001). An efficient local time stepping scheme in adaptive transient computations. Submitted.
- G.R. Richter (1988). An optimal-order error estimate for the Discontinuous Galerkin method. *Math. Comp.*, 50:75–88.
- B. Rivière and M.F. Wheeler (2002). A posteriori error estimates and mesh adaptation strategy for discontinuous Galerkin methods applied to diffusion problems. *Computers and Mathematics with Applications*. to appear.
- B. Rivière, M.F. Wheeler and V. Girault (1999). Improved energy estimates for interior penalty, constrained and discontinuous Galerkin methods for elliptic problems. Part I. *Comp. Geosci.*, 3:337–360.
- R. Sanders (1983). On convergence of monotone finite difference schemes with variable spacing differencing. *Math. Comp.*, 40:91–106.
- A.I. Shestakov, J.L. Milovich and M.K. Prasad (2001). Combining cell- and point-centered methods in 3D, unstructured-grid hydrodynamics codes. *J. Comput. Phys.*, 170:81–111.
- A.I. Shestakov, M.K. Prasad, J.L. Milovich, N.A. Gentile, J.F. Painter and G. Furnish (2000). The radiation-hydrodynamic ICF3D code. *Comput. Methods Appl. Mech. Engrg.*, 187:181–.
- C.-W. Shu (1988). TVD time discretizations. *SIAM J. Sci. Stat. Comput.*, 9:1073–1084.
- C.-W. Shu and S. Osher (1988). Efficient implementation of essentially non-oscillatory shock-capturing methods. *J. Comput. Phys.*, 77:439–471.

- E. Süli and P. Houston (2002). Adaptive Finite Element Approximation of Hyperbolic Problems. In Barth, T. and Deconink, H., editors, *Error Estimation and Adaptive Discretization Methods in Computational Fluid Dynamics*, volume 25 of *Lecture Notes in Computational Science and Engineering*, pages 269–344. Springer Verlag, Berlin.
- J. J. W. van der Vegt and H. van der Ven (1998). Discontinuous Galerkin Finite Element Method with Anisotropic Local Grid Refinement for Inviscid Compressible Flows. *J. Comput. Phys.*, 182:46–77.
- J. J. W. van der Vegt and H. van der Ven (2002a). Slip flow boundary conditions in discontinuous Galerkin discretizations of the Euler equations of gas dynamics. In *Fifth World Congress on Computational Mechanics, July 7-12, Vienna, Austria*.
- J. J. W. van der Vegt and H. van der Ven (2002b). Space-Time Discontinuous Galerkin Finite Element Method with Dynamic Grid Motion for Inviscid Compressible Flows: I. General Formulation. *J. Comput. Phys.*, 182:546–585.
- H. van der Ven and O.J. Boelens (2003). Towards affordable CFD simulations of rotors in forward flight, A feasibility study with future application to vibrational analysis. In *59th American Helicopter Society Forum, May 6-8, Phoenix, Arizona, NLR-TP-2003-100*.
- H. van der Ven and J. J. W. van der Vegt (2002). Space-Time Discontinuous Galerkin Finite Element Method with Dynamic Grid Motion for Inviscid Compressible Flows: II. Efficient flux quadrature. *Comput. Methods Appl. Mech. Engrg.*, 191:4747–4780.
- B. van Leer (1974). Towards the ultimate conservation difference scheme, II. *J. Comput. Phys.*, 14:361–376.
- B. van Leer (1979). Towards the ultimate conservation difference scheme, V. *J. Comput. Phys.*, 32:1–136.
- T.C. Warburton (1998). *Spectral/hp methods on polymorphic multi-domains: Algorithms and Applications*. PhD thesis, Brown University.
- M. Wierse (1997). A new theoretically motivated higher order upwind scheme on unstructured grids of simplices. *Adv. Comput. Math.*, 7:303–335.
- P. Woodward and P. Colella (1984). The numerical simulation of two-dimensional fluid flow with strong shocks. *J. Comput. Phys.*, 54:115–173.
- L. Yin, A. Acharya, N. Sobh, R.B.Haber and D.A.Tortorelli (2000). A space-time discontinuous Galerkin method for elastodynamic analysis. In Cockburn, B., Karniadakis, G., and Shu, C.-W., editors, *Discontinuous Galerkin Methods. Theory, Computation and Applications*, volume 11 of *Lecture Notes in Computational Science and Engineering*, pages 459–464, Berlin. Springer Verlag.